7345-PH-01

Quantum Optical Sources In Photonic Band Structures

Final Technical Report

by

Prof. Gershon Kurizki

July 1995

United States Army

EUROPEAN RESEARCH OFFICE OF THE U.S. ARMY

London England

CONTRACT NUMBER N 681194C 9081

USARDSG-UK

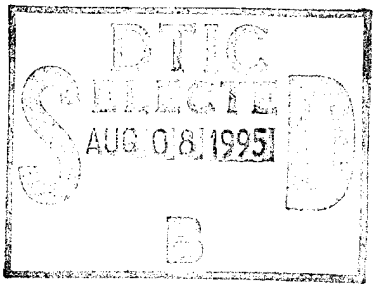

Approved for Public Release; distribution unlimited

REPORT DOCUMENTATION PAGE

Form Approved
OMB No. 0704-0188

1. AGENCY USE ONLY (Leave blank)	2. REPORT DATE	3. REPORT TYPE AND DATES COVERED
	June 30, 1995	Final Report, June 94-June 95

4. TITLE AND SUBTITLE

Quantum Optival Sources in Photonic Band Structures

5. FUNDING NUMBERS

Contract N 681194C
9081
Code N 68171-L

6. AUTHOR(S)

Professor Gershon Kurizki

7. PERFORMING ORGANIZATION NAME(S) AND ADDRESS(ES)

Department of Chemical Physics
Weizmann Institute of Science
Rehovot, 76100
ISRAEL

8. PERFORMING ORGANIZATION REPORT NUMBER

9. SPONSORING/MONITORING AGENCY NAME(S) AND ADDRESS(ES)

USARDSG-UK
Fiscal Office/Edison House
223 Old Marybone Road
London NW1 5TH, England

10. SPONSORING/MONITORING AGENCY REPORT NUMBER

11. SUPPLEMENTARY NOTES

The research report in this document has been made possible through the support & sponsorship of the US Government through its European Office of the US Army.

12a. DISTRIBUTION/AVAILABILITY STATEMENT

12b. DISTRIBUTION CODE

13. ABSTRACT (Maximum 200 words)

See enclosed

14. SUBJECT TERMS

Quantum optical sources, photonic bands

15. NUMBER OF PAGES

16. PRICE CODE

17. SECURITY CLASSIFICATION OF REPORT	18. SECURITY CLASSIFICATION OF THIS PAGE	19. SECURITY CLASSIFICATION OF ABSTRACT	20. LIMITATION OF ABSTRACT
Unclassified	Unclassified	Unclassified	UL

Abstract

The advent of 3D-periodic dielectric structures possessing photonic band gaps (PBGs) and the ability to incorporate defects in the structure, wherein localized high-Q modes are formed at PBG frequencies, should offer far greater control over (i) the spatial modulation of the field amplitude, and (ii) the spectral distribution of its mode density. We have been exploring the following novel quantum optical processes which rely on the "design" of the aforementioned field characteristics in PBG structures: (a) *Quantum states via nonadiabatic periodic transitions:* Unusual nonadiabatic dynamics of field-dressed atomic states is obtained for atoms moving along a near-resonant periodically-modulated field mode. Such dynamics, followed by measurement of the atomic excitation, permits an extremely powerful control over the photon-number and phase distributions of the field. (b) *Pump-mode Fock-state generation:* Atomic states dressed by the defect field can decay via coupling to the mode continuum into a state, which upon measurement of the atomic state, corresponds to a single Fock state of the field. (c1) *Lasing without inversion – atomic coherence by spontaneous decay:* Spontaneous decay of an atom whose resonance is located between two PBGs is found to produce coherence between adjacent atomic sublevels. This coherence can be used to generate electromagnetically-induced transparency, lasing without inversion and nonclassical light. (c2) *Two-atom interactions and coherence:* We predict drastic suppression or enhancement of the resonant excitation transfer and the cooperative frequency shift in systems of two identical atoms placed within PBG structures, both at *near-zone* and *far-zone* inter-atom separations. These effects stem from the competition of PBG-induced single-atom spectral shifts and the inter-atom resonant dipole-dipole interaction. The resulting two-atom stable correlated states can be used for lasing without inversion. (d) *Near-resonant gap solitons and optical "excitons":* We demonstrate that pulse transmission through near-resonant media embedded in 1D-periodic dielectric structures can yield a novel type of gap solitons, which allows for *near-resonant* self-induced transparency at PBG frequencies. At the QED level, we predict the existence of multiphoton bound states, which are the optical analogs of multi-excitons at PBGs of nonlinear periodic structures.

Keywords: Photonic band structures, quantum optics, quantum state preparation, lasing without inversion, cooperative (collective) effects, coherence effects, gap solitons.

I. QUANTUM FIELD STATES VIA NON-ADIABATIC TRANSITIONS

A. Background

PBG structures are expected to allow better control over one of the basic properties that determine the field-atom interaction, i.e., the spatial volume and shape of narrow-linewidth (high-Q) modes. Many of the investigated structures are composed of void spaces periodically alternating with dielectric material. Atomic beams collimated to a micron-size waist can therefore pass through void channels in structures possessing PBGs at near-infrared wavelengths. The resulting field-atom interactions are expected to extend the scope of QED processes realizable in the regime of a *single high-Q mode* near resonance with atomic transition, reversible energy exchange is obtainable between the atom and field. In the simple case of an atom traveling in a *spatially uniform* high-Q mode, this exchange is described by the fundamental Jaynes-Cummings model (JCM) [1,2]. Atomic motion through a *periodically modulated* high-Q mode, in a Fabry-Perot resonator or a defect at a PBG frequency, has been predicted to drastically modify the *resonant JCM dynamics*, and, as shown by us, allow better control over the generation of sub-Poissonian photon statistics in such a mode [3]. In the present study, we have posed the question: can photon statistics and other nonclassical properties of the field be better controlled by *near-resonant* periodic modulation of the field-atom coupling?

B. Results

A novel mechanism for generating nonclassical field states has been discovered (item 6 – Sec.V). based on non-adiabatic periodic modulation of the parameters governing the field-atom coupling. This mechanism has been investigated in the context of a two-level atom moving along a spatially-periodic near-resonant field mode in a PBG structure, resulting in temporal periodicity of the Rabi frequency. We have shown that *steady growth* with number of periods is possible for the field-dressed atomic transition probability. Such steady growth (parametric amplification) is obtained whenever the probability amplitudes in a single period *interfere constructively*, which corresponds to the adiabatic modulation phase in each period being an integer multiple of π.

An advantageous property of such system is the possibility of selective generation of *specific* nonclassical states of the field: (a) For an atom interacting with a spatially sinusoidal quantized field, the possibility of strong enhancement of the transition probability (by constructive interference at many nodes of the field) is very sensitive to the number of photons in the quantized field. Hence, the transition amplitudes may *interfere constructively* only for certain photon-number states. Thus a successful measurement of the atomic excitation results in nearly a Fock state of the field, if only one photon number satisfies the constructive interference condition for the transition. The regime in which several number states are singled out from the initial distribution by the constructive interference and the atomic-excitation measurement results in the generation of amplitude or phase *squeezed states*. (b) The periodic modulation of the field-atom detuning controlled by sufficiently many parameters gives us the possibility to generate an *arbitrary* preselected superposition of photonic

number states (quantum state engineering). The number of components in the preselected superposition is determined by the number of control parameters (Appendix A).

II. PUMP-MODE FOCK-STATE GENERATION BY RESONANCE FLUORESCENCE IN PHOTONIC BAND STRUCTURES

A. Background

Resonance fluorescence (RF) is the emission or scattering of photons into a mode continuum by a two-level atom which is driven by a near-resonant single-mode field [4]. This has been one of the most extensively studied processes in quantum optics, through which several fundamental features of field-atom interaction have been revealed, such as the Mollow triplet spectrum [5] and nonclassical field correlations, manifested by antibunching [6], quadrature squeezing [7] and sub-Poissonian photon statistics [8]. More recently, the interest in RF has shifted to its modifications, taking place when the mode continuum, into which the driven atom radiates,differs from ordinary free-space vacuum. Thus, a squeezed "vacuum" continuum, in which one field quadrature of pairwise-correlated modes exhibits reduced quantum fluctuations, has first been shown to affect spontaneous decay [9], and subsequently has been demonstrated to modify the Mollow-triplet peaks, depending on the squeezing bandwidth ("coloring" of fluctuations) and the phase between the squeezed vacuum and coherent driving fields [10]. Analogous modifications of RF have been revealed in resonator structures with "coloring" of the continuum mode density [11]. These modifications are expected to be especially dramatic in periodic dielectric structures that exhibit photonic band gaps (PBGs), i.e., forbidden spectral bands at all emission angles [12]. For a nearly-classical non-depleted driving field, the inhibition of one of the Mollow triplet spectral sidebands by a PBG has been shown to inhibit the other sideband, thereby causng the disappearance of antibunching [11]. The latter phenomenon has been analyzed using the common assumption of locally-Markovian response of the mode continuum. On the other hand, studies of spontaneous decay into strongly colored continua [13] indicate that non-Markovian features may become prominent near an abrupt, nonanalytic cutoff of the continuum, in a resonator or a periodic dielectric structure. One such feature is the formation of a non-decaying photon-dressed atomic state in the forbidden band [14–16].

B. Results

In recent months [17] (Item 1 – Sec.V) we have studied the dynamical effect of RF on the photon statistics and correlations of the driving field, which undergoes depletion via dressed-state decay near abrupt PBG edges. The most striking outcome of this process is that an initially broad (Poissonian or thermal) photon-number distribution of the driving field can become highly sub-Poissonian, with a narrow peak about a single Fock state, following a measurement of the atomic excitation. The realization of such distributions may therefore be a major stepping stone towards the construction of novel quantum light sources, including photon-number states. We also show that the dressed-state non-diagonal matrix elements yield, upon measuring the atomic state, coherences between Fock states of the field. Hence,

the two predominant "attractor" states, say, $|n_0\rangle$ and $|n_0 - 1\rangle$, whenever the defect mode is shifted from the PBG center, will be *partly correlated*, if an initial coherence exists either in the atom or in the field. Therefore deviations from *phase randomness* of the field are anticipated.

Another striking effect of the stable (non-decaying) dressed-state coherences is the appearance of *beats (oscillations) of Fock-state populations of the field prepared by measuring the final atomic state.* These oscillations will be strongly pronounced in the case when the initial photon distribution spans many PBGs in the spectral density of modes (DOM). In this case the field distribution will consist of many partly-correlated Fock states [17].

III. LASING WITHOUT INVERSION:

III.1 Single-Atom Systems

A. Background

If the lower state of the resonant atomic transition consists of two sublevels $|g\rangle$ and $|g'\rangle$ a Λ-configuration), then the atomic state coherence $\rho^0_{gg'}$ can be used in a scheme of lasing without inversion(LWI) between the $|g\rangle - |g'\rangle$ doublet and a higher atomic level $|u\rangle$. It has been long known that, if the single-photon Rabi frequency of a cavity mode, Ω_1, is much larger than its linewidth Γ_1, then the dressed atomic state will be split after time $\sim \omega_1^{-1}$ into a nearly-equal superposition of two dressed states whose energies ω_1 and ω_2 are pushed in opposite directions from the cavity-mode peak by roughly $\pm\Omega_1/2$. We have posed the question: can we base LWI schemes on similar, spontaneously induced coherence in PBG structures? (Item 7 – Sec.V).

B. Results: Spontaneous Coherence Formation in PBG Structures

Assume that the transition between a ground $|g\rangle$ and an excited $|e\rangle$ levels of the atom is near resonant with a narrow photonic band. The band is assumed to be well separated from other bands, so that the influence of the latter can be neglected. Moreover, the band is assumed to be sufficiently dense and narrow, i.e.,

$$G_m \gg \Delta_b,\ |\Delta_m|, \tag{1}$$

where G_m and Δ_b are the maximum value and the width of the function $G(\omega)$ characterizing the stregth of the atom-band coupling, $\Delta_m = \omega_a - \omega_m$, ω_m is the center of gravity of the band,

$$\omega_m = \frac{1}{A}\int_{\omega_U}^{\omega_L} d\omega\omega G(\omega), \tag{2}$$

ω_U and ω_L are the lower and upper band edges respectively, and

$$A = \int_{\omega_U}^{\omega_L} d\omega G(\omega). \tag{3}$$

Then the level e can be shown [16] to split to two levels 1 and 2, whose separation to first approximation is

$$E_2 - E_1 = \hbar\sqrt{4A + \Delta_m^2} = \hbar\Omega_R, \tag{4}$$

where Ω_R is the vacuum Rabi frequency. An excited atom injected at $t = 0$ into the PBS in the case (1) undergoes an insignificantly small spontaneous decay over a time of order $1/\Omega_R$, after which the excited-state wavefunction becomes a *coherent superposition* of the states $|\psi_1\rangle$ and $|\psi_2\rangle$ [16],

$$|\Psi(t)\rangle = \sqrt{c_1}|\psi_1\rangle e^{-i\omega_1 t} + \sqrt{c_2}|\psi_2\rangle e^{-i\omega_2 t}, \tag{5}$$

where $\omega_j = E_j/\hbar$. If there is a nonzero matrix element of the dipole moment, d_{3e}, for the transition between the level e and another level 3, then the dipole moment matrix elements for the transitions 1-3 and 2-3 are given by

$$d_{31} = \sqrt{c_1}d_{31}, \qquad d_{32} = \sqrt{c_2}d_{3e}. \tag{6}$$

For the near-resonant case, $\Delta_m^2 \ll 4A$, which is of special interest here, one gets in the first approximation

$$c_1 = c_2 = \frac{1}{2}, \qquad \omega_{1,2} = \frac{\omega_a + \omega_m}{2} \mp \sqrt{A}. \tag{7}$$

The density matrix elements of the system consisiting of the levels 1 and 2 are [cf. Eqs. (5) and (7)]

$$\rho_{11}(t) = \rho_{22}(t) = \frac{1}{2}, \qquad \rho_{12}(t) = \rho_{21}^*(t) = \frac{e^{2i\sqrt{A}t}}{2}. \tag{8}$$

C. Results: Lasing Without Inversion

The coherence between the levels 1 and 2 can be utilized to produce lasing without inversion [18]. Following Refs. [19–21], consider a Λ-system. The field

$$E(t) = E_0 e^{-i\omega t} + \text{c.c.} \tag{9}$$

couples the upper level 3 with the lower levels 1 and 2. The levels 1, 2, and 3 have have the reciprocal lifetimes respectively γ_1, γ_2, and $\gamma_3 = \gamma_{31}' + \gamma_{32}' + \gamma_3'$, where γ_{31}', γ_{32}', and γ_3' are the spontaneous rates of transitions from the level 3 to the levels 1, 2, and all others respectively, whereas the reciprocal lifetimes of the coherences ρ_{12} and ρ_{13} are γ_{21} and γ_{31} respectively. The levels 1 and 2 can have finite lifetimes due to one or several of the following factors: spontaneous transitions to levels other than the ground state, finite time of presence of the atom in the structure, finite density of modes outside the narrow band (which causes the splitting of the level e), and collision-induced transitions. The open 3-level sysytem is described here by an unnormalized density matrix $R(t)$, whose diagonal elements yield the number of atoms in the laser cavity in the respective level.

Our results show that a spontaneously-formed coherent superposition of the states 1 and 2 allows only a very small fraction of atoms in these states to absorb the field $E(t)$. Therefore there can be gain whenever the number of the atoms at the level 3 is much less than the number of the atoms at the lower levels 1 and 2 and $\omega_{12} \gg \gamma_{21}, \gamma_{31}$ (Appendix B).

III.2 Two-Atom Effects

A. Background

Studies of cooperative atomic effects in resonantors have been extensions of the Tavis-Cummings model [22]. This model assumes many atoms identically coupled to a single mode and ignores the symmetry-breaking dipole-dipole effects, which are important at near-zone separations [23,24].

Our study is aimed at gaining new insight into cooperative effects: a pair of identical two-level atoms (or excitons), sharing a photon with one or many high-Q modes in a photonic-band structure or resonator. Such effects may be important for the spontaneous formation of *coherence* in two-atom systems and its utilization for *lasing without inversion* (see above). We have developed a formalism capable of treating two atoms coupled to a field with an *arbitrary* mode-density spectrum in *a non-perturbative fashion.* Such a formalism is necessary because the standard perturbative treatment of two-atom coupling, to second order in the field [25], is *inadequate* for a reservoir whose mode-density spectrum does not vary smoothly, as demonstrated already by our comprehensive theory of a single atom coupled to such a reservoir [16].

B. Results

Our treatment (Item 4 Sec.V) demonstrates that two identical atoms interacting via a near-resonant narrow-linewidth mode (or degenerate band) and an off-resonant reservoir can exhibit a much richer variety of spectral and dynamical features than what is currently known. It must be viewed as a system of *three* mutually coupled excited states (as opposed to *two* such states in previously studied models [25,22]). The dipole-dipole (RDDI) coupling and the mode-induced Rabi splitting are *inseparable* in this system. The interatom coupling results from mixing of all three states, which is most striking for separations where the two predominantly-populated levels nearly cross. Then the competing RDDI and Rabi splittings cause strong interference of the symmetric and antisymmetric two-atom excited states, leading to *decoupling* of single-atom excited states. This occurs at near-zone (quasimolecular) separations (as small as $10^{-2}\lambda_A$) and corresponds to *suppression* of interatom excitation transfer, compared to the electrostatic near-zone limit of RDDI.

The present predictions, particularly the suppression of excitation transfer at quasimolecular separations, may be important in various systems of two atoms, molecules, or excitons within high-Q Bragg resonators (Appendix C).

IV. PROPAGATION EFFECTS

IV.1 Self-Induced Transparency in Photonic Band Structures: Gap Solitons Near Absorption Resonances

A. Background

Pulse propagation in a non-uniform resonant medium, e.g., a periodic array of resonant films, can destroy self-induced transparency (SIT) [26,27], because the pulse area is then split between the forward and backward (reflected) coupled waves, and is no longer conserved [28,29]. Should we then anticipate severely hampered transmission through a medium whose resonance lies in a reflective spectral domain (photonic band gap) of a periodically-layered structure (a Bragg reflector)? We have shown analytically [30] (Item 2 – Sec.V) that it is possible for the pulse to overcome the band-gap reflection and produce SIT in a near-resonant medium embedded in a Bragg reflector. The predicted SIT propagation is a *principally new type of a gap soliton*, which does not obey any of the familiar soliton equations, such as the non-linear Schrödinger equation (NLSE) or the sine-Gordon equation. Its spatio-temporal form and intensity dependence are shown here to be distinct from the extensively – studied gap solitons in Kerr–non-linear Bragg reflectors, which are described by the NLSE.

B. Results

In treatments of bidirectional field propagation in media with arbitrary spatial distribution of near-resonant atoms [31,32], the Bloch equations for the population inversion and polarization are entangled in a fashion which leads to an infinite hierarchy of equations for successive spatial harmonics. Here we avoid this complication by confining the near-resonant two-level systems (TLS) to layers much thinner than the resonant wavelength, with the same periodicity as the dielectric structure.

Our main idea has been to try the following phase-modulated 2π–soliton SIT solution for the envelope of the forward (F) and backward (B) field

$$E_{F(B)} = \frac{\hbar}{2\mu\tau_c}\left(1 \pm \frac{1}{u}\right) A_0 \frac{\exp\left[i(\alpha n_0 z/c\tau_c - \Delta t)\right]}{\cosh\left[\beta(z/\tau_c cu - t)\right]} \tag{10}$$

where μ is the transition dipole moment, τ_c is the cooperative (resonant) absorption time, A_0 is the amplitude of the solitary pulse, u is the velocity (normalized to c), n_0 is the mean refractive index and Δ is the field detuning from the gap center.

We focus here on the most illustrative case, when the TLS resonance is exactly at the center of the optical gap. Then the phase modulation α, the pulse inverse-width $\beta = A_0/2$ and the detuning Δ are analytically obtainable as a function of the group velocity cu. We find that the condition for SIT is that the cooperative *absorption length* $c\tau_c/n_0$ should be *shorter than the reflection* (attenuation) *length* at the gap $1/\kappa$, i.e., that the incident light should be absorbed by the TLS before it is reflected by the Bragg structure. SIT is found to exist only on one side of the band-gap center, depending on whether the TLS are embedded in the region of higher or lower linear refractive index in the Bragg structure. This result may be understood as the addition of a near-resonant non-linear refractive index to the

modulated index of refraction of the Bragg structure. When this addition compensates the linear modulation, then there is no band gap and soliton propagation is possible. The soliton amplitude dependence on frequency detuning from the gap center (which coincides with the TLS resonance) is shown The parameters obtained from our analytical solutions fully agree with those which yield both forward and backward soliton-like pulses in a numerical simulation of Maxwell-Bloch equations.

An adequate system for experimental observation of this effect appears to be a periodic array of 12-nm–thick GaAs quantum wells ($\lambda = 806$nm) separated by $\lambda/2$ non-resonant Al-GaAs layers. Area density concentration $\sigma \sim 10^8$–10^9 cm^{-2} of the quantum-well excitons yields $\tau_c \simeq 10^{-13}$–10^{-14}s. A solitary pulse of $\leq$ 1ps, i.e., much shorter then the dephasing time $T_2 \sim 10$ps (at 2^0K) in this structure requires band-gap reflection length $1/\kappa \geq 100\ \lambda$.

The salient advantage of the predicted near-resonant gap soliton is stability with respect to absorption. By contrast, strong absorption is a severe problem associated with a large Kerr coefficient required for NLSE gap solitons (Appendix D).

IV.2 Theory of Quantum Gap Solitons

A. Background

By nature any dielectric material is nonlinear. The nonlinearity changes the PBG properties of periodic structures to some degree. In one-dimensional (1D) photonic crystals, even weak nonlinearity acts as a large perturbation on these properties. In recent years it has been shown that 1D Kerr-nonlinear photonic crystals admit band-gap solitary waves, which are called gap solitons. Current studies correspond to classical gap solitons. Since quantum many-body properties of light can be important in nonlinear optical processes, we have developed the quantum theory of gap solitons in a 1D Kerr-nonlinear photonic crystal (Item 5 – Sec.V).

B. Results

The basic idea is that incident photons with frequencies in a band gap are scattered by the nonlinearity into the conduction and valence bands of the photonic crystal. The effective Hamiltonian of quantum gap solitons is derived in the two-band effective-mass approximation. The eigenstates of the Hamiltonian are constructed exactly by Bethe's ansatz method. We find that in a certain band gap of the photonic crystal quantum gap solitons can be in bound states, consisting of one or more photon pairs from the valence and conduction bands. Such bound-state quantum gap solitons are optical analogs of exciton molecules. Here we give the $2N$-body bound-state wave function in the unnormalized form

$$\Psi(z_{1\pm},...,z_{N\pm}) \propto \exp\left(\sum_{j=1}^{N} iK\frac{m_-z_{j-}-m_+z_{j+}}{m_--m_+}\right) \times \exp\Big(-\sum_{j=1}^{N}\frac{m_-m_+V_i}{(m_--m_+)\hbar^2}|z_{j+}-z_{j-}| \tag{11}$$

$$- \frac{|V_\alpha|}{\hbar^2} \sum_{j<l} (m_- |z_{j-} - z_{l-}| + m_+ |z_{j+} - z_{l+}|) \Big)$$

The exponential factors in the bound state $|\Phi_{2N}>$ can be revealed by the dependence of the intensity-intensity correlation function $G^{(2)}$ on the separation η of two photon counters detecting the field in the structure:

$$G^{(2)}(\eta) = \int < \Phi_{2N} | \mathcal{E}^+(z) \mathcal{E}^-(z) \mathcal{E}^+(z+\eta) \mathcal{E}^-(z+\eta) | \Phi_{2N} > dz \tag{12}$$

where the operator $\mathcal{E}^-(z) = \phi_+(z) + \phi_-(z)$ is the position-dependent negative-frequency field envelope. The $2N$-body bound-state energy eigenvalues are found to have the following form,

$$E_{2N} = 2N\hbar(\omega_0 \pm \omega_{2N}) \tag{13}$$

$$2\hbar\omega_{2N} = \frac{\hbar^2 K^2}{2|m_- - m_+|} + \frac{m_- m_+ V_i^2}{2|m_- - m_+|\hbar^2} - \frac{|m_- - m_+| V_\pm^2}{6\hbar^2}(N^2 - 1) \tag{14}$$

where $\omega_0 = (\omega_+ + \omega_-)/2$ is the center of the band gap and the upper (lower) sign is chosen according to that of the Kerr nonlinearity. As seen from these equations, bound states are associated with discrete transmission lines at $\Omega_{2N} = \omega_0 \pm \omega_{2N}$ in the band gap.

As a realistic example, we consider a periodic structure of alternating layers of GaAs crystal and linear dielectic. The layer thicknesses are $a_1(\text{GaAs}) = 0.2338$ μm and $a_2 = 0.3044$ μm. The refractive index of GaAs crystal is $n_1 = 3.60$ and the refractive index n_2 of linear dielectric varies from 1.00 to 3.574. GaAs crystal is a self-defocusing medium and has a high nonlinear susceptibility $\chi_1^{(3)} = -2.5482 \times 10^{-10}$ (cm/V)^2 for light frequencies below the bandgap $E_g = 2.1573 \times 10^{15}$ s^{-1}. The calculation reveals that in the second lowest band gap of this structure quantum gap solitons can be in bound states. The numerical results reproduce the multi-exponential fall-off of the intensity-intensity correlation function $G^{(2)}(\eta)$ with the detector separation η and the variation of the optical exciton frequency Ω_{2N} with the relative refractive index n_1/n_2, for different quantum numbers N.

In conclusion, bound-state quantum gap solitons will manifest themselves via distinct dependence of the intensity-intensity correlation function on the detector separation and via transmission resonances at band-gap frequencies (Appendix E).

IV.3 Superluminal Delays of Coherent Pulses in PBG structures

A. Introduction

As shown by a two-photon interference experiment [33], a photon that has tunneled as an evanescent wavepacket through a PBG structure (dielectric-mirror) appears to have been delayed significantly less than its "twin" photon that has traversed the same distance in vacuum. Such a delay has been interpreted as signifying "superluminal" (faster-than-light) barrier-traversal time. Similar "superluminal" time delay in tunneling through a dielectric mirror has now been measured in a classical two-pulse interference experiment [34]. The latter experiment has also revealed a remarkable feature, namely, that the temporal width of the transmitted wavepacket is strongly narrowed down.

It is always possible to trace numerically the evanescent wavepacket evolution and compare its features with different definitions of barrier traversal times [35–40] (see below). Nevertheless, the *mechanism* of superluminal time delays is still obscure [33] and regarded as a "poorly resolved mystery" [40]. A commonly invoked notion is that this mechanism is spectral reshaping (filtering) of the transmitted wavepacket by dispersion. Yet why should spectral reshaping necessarily yield superluminal delays of EM pulses in non-absorbing structures, after propagating in (dispersionless) vacuum? Is there a *common mechanism* for superluminal time delays and wavepacket narrowing, which applies to both EM pulses in dielectric structures and relativistic massive particles in potential barriers [40]? How is causality compatible with superluminal transmission, particularly in the single-photon case [33]?

We purport to show (Item 3 – Sec.V) that the above questions can only be answered by a *universal description* of the temporal wavepacket transmission as *interference between its causally-propagating consecutive components*. Our description reveals, for the first time, the key role of phase coherence in tunneling, by demonstrating its dependence on the *coherence time* (phase randomization) of the wavepacket. An important corrolary is that superluminal time delays can occur also in allowed propagation, namely, propagation which can only be described by *real wavevectors* (e.g., in Fabry-Perot structures) and not only in evanescent-wave tunneling, where complex wavevectors can be employed (e.g., in photonic band-gap structures).

B. Results

Our theory has demonstrated, for the first time, that the universal mechanism of predominantly destructive interference between accessible causal paths is responsible for transmission attenuation, superluminal delay times and wavepacket narrowing. Two other characteristics of evanescent waves ,namely, exponential attenuation and traversal-length independence of the mean traversal time of the structure length [34] can also be explained in terms of this universal mechanism. This theory overcomes the limitations of previous approaches, since it applies to arbitrary pulse shapes, widths and coherence times, and *explicitly* reveals the causal nature of their transmission. The understanding provided by this theory may open new perspectives in the design of the velocity, intensity and shape of transmitted pulses, by manipulating the phase delays along the accessible paths in the medium (Appendix F).

V. PAPERS SUBMITTED FOR PUBLICATION (PARTIAL SUPPORT BY USARDSG):

1. B. Sherman, A. G. Kofman and G. Kurizki "Preparation of nonclassical field states by resonance fluorescence in photonic band structures", *Appl.Phys.B* **60**, S99 (1995) (special issue on fundamental systems).

2. A. Kozhekin and G. Kurizki "Self-induced transparency in Bragg reflectors: Gap Solitons near absorption resonances", *Phys.Rev.Lett* **74**, 5020 (1995)

3. Y. Japha and G. Kurizki "Superluminal delays of coherent electromagnetic pulses: a universal mechanism", *Phys.Rev.A* (in press)

4. G. Kurizki, A. G. Kofman and V. Yudson "Photon Exchange by Atom Pairs in Resonators", *Phys.Rev.A* (submitted)

5. Ze Cheng and G. Kurizki "Optical Multi-Excitons: Quantum Gap Solitons in Nonlinear Bragg Reflectors" *Phys.Rev.Lett* (submitted)

6. B. Sherman *et.al.* "Quantum Field State Preparation via Nonadiabatic Periodic Interaction", (in preparation)

7. A. G. Kofman and G. Kurizki "Lasing without Inversion via Spontaneous Coherence in Photonic Band Structures" (in preparation).

VI. SCIENTIFIC PERSONNEL

Dr. Abraham Kofman
Dr. Ze Cheng
Mr. Boris Sherman (submitted his Ph.D. thesis during the project)
Mr. Alexander Kozhekin (Ph.D. student)
Mr. Yonathan Japha (Ph.D. student)

VII. REFERENCES

[1] J. Eberly, N. Narozhny, and J. Sanchez-Mondragon, Phys. Rev. Lett **44**, 132 (1980).

[2] P. Knight and P. Radmore, Phys. Rev. A **26**, 676 (1982).

[3] B. Sherman, G. Kurizki, and A. Kadyshevitch, Phys. Rev. Lett. **69**, 1927 (1992), G. Kurizki, B. Sherman and A. Kadyshevitch, J. Opt. Soc. Am. B **10**, 346 (1993).

[4] C. Cohen-Tannoudji, J. Dupont-Roc and G. Grynberg, *Atom-Photon Interactions: Basic Processes and Applications* (Wiley, 1992); see also J. D. Cresser, Phys. Rep. **94**, 42 (1983).

[5] B. R. Mollow, Phys. Rev. **188**, 1969 (1969).

[6] H. J. Carmichael and D. F. Walls, J. Phys. B **9**, 1199 (1976).

[7] D. F. Walls and P. Zoller, Phys. Rev. Lett. **47**, 709 (1981).

[8] R. Short and L. Mandel, Phys. Rev. Lett. **51**, 384 (1983).

[9] C. W. Gardiner, Phys. Rev. Lett. **56**, 1917 (1986).

[10] H. J. Carmichael, A. S. Lane and D. F. Walls, Phys. Rev. Lett. **58**, 2539 (1987); A. S. Parkins, Phys. Rev. A **42**, 4352 (1990).

[11] M. Lewenstein, T. M. Mossberg and R. Glauber, Phys. Rev. Lett. **54**, 775 (1987); T. W. Mossberg and M. Lewenstein, Phys. Rev. A **37**, 2048 (1988).

[12] E. Yablonovitch, Phys. Rev. Lett. **58**, 2059 (1987), J. Opt. Soc. Am **B10**, 283 (1993); S.John, Phys. Today 44(5), 32 (1991).

[13] K. Wodkiewicz and J. H. Eberly, Ann. of Phys. **101**, 574 (1976).
[14] B. Fain, Phys. Rev. A **37**, 546 (1988).
[15] S. John and J. Wang, Phys. Rev. B **43**, 12774 (1991).
[16] A. G. Kofman, G. Kurizki, and B. Sherman, J. Mod. Opt. **41**, 353 (1994).
[17] B. Sherman, A. G. Kofman, and G. Kurizk, Appl.Phys.B (special issue on fundamental systems) **60**, S99 (1995).
[18] M. O. Scully, S. Zhu, and A. Gavrielides, Phys. Rev. Lett. **62** , 2813 (1989).
[19] M. O. Scully, Phys. Rev. Lett. **67**, 1855 (1991).
[20] N. Lu, Phys. Rev. A **45**, 5011 (1992).
[21] U. Rathe *et al.*, Phys. Rev. A **47**, 4994 (1993).
[22] M. Tavis and F. W. Cummings, Phys. Rev. **188**, 692 (1969); G. S. Agarwal, Phys. Rev. Lett. **53**, 1732 (1984); M. G. Raizen et al., Phys. Rev. Lett. **63**, 240 (1989).
[23] G. S. Agarwal, *Quantum Statistical Theories of Spontaneous Emission* (Springer, Berlin, 1974).
[24] H. Freedhof, Phys. Rev. A **19**, 1132 (1979); Y. Ben-Aryeh and C.M. Bowden, IEEE J. Quantum Electron. **24**, 1376 (1988); G. V. Varada and G. S. Agarwal, Phys. Rev. A **45**, 6721 (1992).
[25] D. P. Craig and T. Thirunamachandran, *Molecular Quantum Electrodynamics* (Academic, London, 1984).
[26] S. L. McCall and E. L. Hahn, Phys.Rev **183**, 457 (1969).
[27] A. Maimistov, A. Basharov, and S. Elyutin, Phys.Rep. **191**, 2 (1990).
[28] B. I. Mantsyzov and R. N. Kuz'min, Sov. Phys. JETP **64**, 37 (1986).
[29] T. I. Lakoba, Phys. Lett. A **196**, 55 (1994).
[30] A. Kozhekin and G. Kurizki, Physical Review Letters **74** , 5020 (1995).
[31] M. I. Shaw and B. W. Shore, JOSA B **8**, 1127 (1991).
[32] R. Inguva and C. M. Bowden, Phys.Rev.A **41** , 1670 (1990).
[33] A. M. Steinberg, P. G. Kwiat, and R. Y. Chiao, Phys. Rev. Lett. **71**, 708 (1993).
[34] C. Spielmann, A. S. R. Szipöcs, and F. Krausz, Phys. Rev. Lett. **73** , 2308 (1994).
[35] M. Büttiker and R. Landauer, Phys. Rev. Lett. **49**, 1739 (1982).
[36] E. H. Hauge and J. A. Stovneng, Rev. Mod. Phys. **61** , 917 (1989).
[37] D. Sokolovski and L. M. Baskin, Phys. Rev. A **36** , 4604 (1987).
[38] D. Sokolovski and J. N. L. Connor, Phys. Rev. A **47**, 4677 (1993).
[39] H. A. Fertig, Phys. Rev. A **47** , 4677 (1993).
[40] T. Martin and R. Landauer, Phys. Rev A **45**, 2611 (1992).

Appendix A:
Non-Classical Field States via Periodically Non-Adiabatic transitions

B. Sherman, G. Kurizki and A. Kozhekin
V. Akulin[†] and A. Levine[‡]
Chemical Physics Department, Weizmann Institute of Science, Rehovot 76100 Israel

A novel mechanism for generating nonclassical field states has been discovered, based on non-adiabatic periodic modulation of the parameters governing the field-atom coupling.

The resonant interaction of a quantized field with a two-level atom has been intensively studied in single-mode resonators where the atomic motion plays no role, since the field is taken to be spatially uniform in the beam direction. The field-atom interaction then conforms to the fundamental Jaynes-Cummings model [1,2] (JCM).

Our purpose here is to show that atomic motion along a cavity mode can give rise to new QED effects that originate from the spatial character of the field. These effects can be revealed by propagating an atomic beam through a cavity along its axis or through a defect in a photonic crystal [3].

It has been shown that periodic temporal modulation of the *resonant* field-atom coupling for an atom moving along a standing-wave mode can drastically modify the prominent dynamical features of the JCM [1,2], such as (a) the evolution of "Schrödinger cats" and their photon statistics [4]; (b) the corresponding oscillations of the atomic population inversion [5]. Hear we show that *near-resonant* oscillatory modulation of the coupling in the same system gives rise to even more dramatic modifications of atomic and field dynamics. In addition to their inherent novelty and interest, these modified dynamical features are shown to allow much better control than their JCM counterparts over the generation of nonclassical field states.

The system under consideration involves the classical translational motion of the atom, the internal atomic states, and the quantized EM field. The atomic internal states become strongly entangled with the quantized field state in the course of their interaction. The resulting combined field-atom system has eigenenergies and eigenstates ("dressed states"). The dressed-state energies depend on the field amplitude and therefore on the atomic location within the field mode. In the limit of slow atomic motion along a standing-wave field mode, the field-atom system adiabatically follows the dressed state associated with the instantaneous atomic position. However, the system can still undergo non-adiabatic transitions from one dressed state to another, with exponentially small probability. In this case, the kinetic energy of the classically-moving atom is transferred to the internal quantum degrees of freedom of the combined field-atom system. Such a non-adiabatic transition is very unlikely for sufficiently slow atoms, and therefore it occurs near the field nodes, where the energy required for such a transition is minimal (see Fig.1). Since the transition can occur at any of the nodes along the atomic path, the amplitudes of the transitions at different nodes interfere. The phases of these interfering amplitudes are very sensitive to the number of photons in the quantized field. Hence, only for several photon-number states the

amplitudes may *interfere constructively*, significantly contributing to the probability of the non-adiabatic transition. This implies that non-adiabatic transitions are strongly correlated with certain photon-number states. Therefore, a measurement that finds an atom-field system, which was initially prepared in the lower dressed state, in the upper dressed state (which almost coincides with the atomic ground state in the case of large detuning $\Delta = \omega_a - \omega$), projects the initial field distribution on these number states out. The final field statistics is the convolution of the initial one with the weights of different photon numbers in the non-adiabatic transition probability.

The Hamiltonian for a two-level atom with dipole-transition frequency ω_a moving through the electromagnetic field of a spatially periodic mode with frequency ω reads

$$\hat{H} = \hbar\omega_a \frac{\hat{\sigma}_3}{2} + \hbar\omega\hat{a}^\dagger\hat{a}\hbar\Omega[\vec{r}(t)](\hat{\sigma}_+\hat{a} + \hat{a}^\dagger\hat{\sigma}_-). \tag{1}$$

Here $\hat{\sigma}_+(\hat{\sigma}_-)$ and $\hat{a}^\dagger(\hat{a})$ are the atomic and field raising (lowering) operators, respectively, whereas the coupling strength $\Omega(\vec{r})$ depends on the amplitude of the field mode $\mathcal{E}$ at a given point

$$\hbar\Omega[\vec{r}(t)] \;=\; (\hbar\omega/2)^{1/2}\;(\vec{\mu}\cdot\hat{\epsilon}_\lambda)\,\mathcal{E}\;(z \;=\; \vec{v}t \;+\; \vec{r}_\perp) \tag{2}$$

. where $\vec{\mu}$ is the atomic dipole moment and $\hat{\epsilon}_\lambda$ is the mode polarization.

We consider classical translational motion of an atom with the constant velocity $\vec{v}$ along the nodes of the mode in a structure of length l. We assume that the kinetic energy of the atom is much bigger than the energy of the non-adiabatic transition, such that the dispersion of the wave packet due to the velocity difference after and before the the transition are much smaller than the atom's size, that is $\hbar\Delta/mv^2 \gg R_{at}/l$. This condition is satisfied, for example, for a cesium atom with velocities of $10^4 cm/s$ and non-adiabatic transition frequency Δ of $10^7 s^{-1}$ moving through a resonator with a length l of $1cm$.

For an atom moving in a sinusoidally periodic mode with period λ the amplitude $\mathcal{E}(z)$ can be chosen to be real, here we can write

$$\Omega[z(t)] = \Omega_0 \sin(2\pi t/T), \tag{3}$$

with $T = \lambda/v$.

The Hamiltonian (1) has two adiabatic energy terms

$$\epsilon_n^\pm(t) = \hbar\omega(n+1) \pm \hbar\sqrt{\Delta^2(t)/4 + \Omega^2(t)(n+1)}. \tag{4}$$

In the limit of vanishingly small atomic velocity, the evolution of $\epsilon_n^\pm(t)$ is adiabatic, i.e., if initially the atom was in the eigenstate with energy $\epsilon_n^-(0)$, then, after time t, the eigenstate acquires an adiabatic phase factor $\exp[-i\int_0^t \epsilon_n^-(t')dt'/\hbar]$ Thermal velocity v of the off-resonant atom results in weak non-adiabaticity, if the Doppler frequency $\omega_D = 2\pi/T = (2\pi/\lambda)v$, is small in comparison with the atom-field detuning $\Delta = \omega_a - \omega$, $\Delta \gg \omega_D$. Non-adiabatic transitions are possible only in the vicinity of the points of the energies closest approach [6], namely, where $\Omega(t) = 0$ (see Fig.1). In order to find the probability amplitude of such a transition, one can in principle use the first order approximation in the non-adiabatic coupling [7]. However, since the result is exponentially small, the first order approximation

in the non-adiabatic coupling yields *incorrect* result [8]. A more precise expression for the amplitude of the transition a_n is derived by Dykhne [8].

$$a_n = \exp\left[Im \oint_0^{t_c} dt\sqrt{\Delta^2 + 4\Omega^2(t)(n+1)}\right], \tag{5}$$

where t_c is the branching point of the integrand (the points of levels crossing) in the complex time plane, that is closest to the $Re\ t$ axis.

In this approximation the non-adiabatic transitions are sudden jumps at the nodes of the standing wave. The phase difference for transitions at two adjacent transition space-points reads

$$2\varphi_n = \int_0^T dt\sqrt{\Delta^2 + 4\Omega_0^2(n+1)\sin^2\omega_D t}, \tag{6}$$

and results in the following net amplitude of the non-adiabatic transition after K nodes the atom has passed

$$A_n = e^{-iK\varphi_n} a_n \sum_{l=0}^{K} e^{il\varphi_n} = a_n \frac{\sin K\varphi_n}{\sin\varphi_n}. \tag{7}$$

Since the probability of the non-adiabatic transition is small, we neglect processes with more than one net jump (the next nonvanishing order of approximation would involve *triple* jumps — from the lower to the upper state, then down to the lower state and finally back to the upper state).

We now consider the field evolution and assume that the atom has been initially prepared in its ground state $|g\rangle$, that is

$$|\psi(0)\rangle = \sum_n c_n |n+1\rangle|g\rangle. \tag{8}$$

The atom is taken to start and finish its motion at the nodes, where $\Omega = 0$ and the ground and excited states are the lower and upper dressed states, respectively. Hence, if after the interaction with the field the atom is found in the upper state, this means that the non-adiabatic transition has definitely happened. The field-atom final wavefunction, reduced by the conditional measurement of atomic excitation is

$$|\psi(t = KT)\rangle = N\sum_n c_n A_n e^{in\omega KT}|n\rangle|e\rangle, \tag{9}$$

where N is the normalization factor. We see from (9) that the resulting field statistics is the convolution of the transmission function A_n and the initial photon distribution c_n. This can result in selecting ("filtering") out either a single or several number state components, with the corresponding phases, thus generating a strongly non-classical state. We can adjust A_n over a wide range of possibilities via the following dimensionless parameters: $\eta = \Delta^2/4\Omega_0^2$, $\xi = \Omega_0/\omega_D$ and the number of nodes of the standing wave K. The net amplitude A_n has narrow peaks corresponding to *the constructive interference condition* on the adiabatic phase difference (6).

$$\varphi_n = \pi m,\ m = 1, 2, 3.... \tag{10}$$

Under this condition, the multichannel constructive interference enhances the transition probability by K^2. If only one photon number produces the peak, which contributes to the convolution (9) with the initial field distribution, then the final field state becomes nearly a Fock state (see Fig.2) after the conditional measurement of the atomic excitation. Thus a *presecelected* Fock-state is generated.

Consider now the opposite case of wide range of n satisfying the constructive interference condition (10) and, therefore, contributing to the convolution (9). We assume that: (i) the adiabatic phase difference $\varphi_n \sim \sqrt{n}$, (ii) a_n do not vary strongly with n. This means that one gets the convolution of the initial filed statistics with the sine of $\sqrt{n}$, which is typical to one-photon JCM [1,2]. As it was shown [9–11] for a field, initially prepared in a quasiclassical coherent state a conditional measurement leads to the formation of a *macroscopic quantum superposition* of two nearly-coherent states with identical mean amplitudes (same as the initial one) and different mean phases ("Schrödinger cat"). The corresponding Q-function and the phase distribution $F(\phi)$, described in the Pegg-Barnett formalism [12] by the function

$$F(\phi) = \frac{1}{2\pi}\left|\sum_n c(n)e^{-in\phi}\right|^2 \tag{11}$$

are shown in Fig.3.

The intermediate regime, when several number states are singled out from the initial distribution by the constructive interference and the conditional measurement (CM) of the atom in $|e\rangle$, results in the generation of *amplitude squeezed states* similar to the ones predicted by Yamamoto et al. for strong self-squeezing in Kerr media [13] (see Fig.4).

The weakly-nonadiabatic regime considered above imposes two major limitations on non-classical field-state preparation via constructive interference of nonadiabatic transitions followed by a CM of the atom: (i) the CM success probability is typically low ($\sim 1\%$); (ii) the resulting Fock-state amplitudes are controlled by very few parameters, which restricts the type of field state that can be prepared. In order to overcome these limitations, we adopt the model of temporal Kronig-Penney modulation, e.i. , periodically alternating abrupt jumps of the field detuning Δ or coupling constant (Fig.5). Then the nonadiabatic transition probability is *large* in every cycle of the modulation. This type of modulation can be achieved in photonic band structures [3], when the mode frequency is near the forbidden gap edge. Under the condition of constant atomic velocity, the atom-field coupling is modulated with period $T = t_F + t_D$, where t_F is the *duration of the zero-coupling stage* ($\Delta \gg \omega_D, \Omega_0$), and t_D is the duration of the 'dressed' evolution ($\Delta \sim \Omega_0$). The 2×2 evolution matrix of the first stage is diagonal, it describes the free oscillations of atom+field states with appropriate energies

$$\hat{U}_F(t_F) = \exp[-i(\omega\hat{a}^\dagger\hat{a} + (\omega - \Delta)\hat{\sigma}_3/2)t_F] = e^{-i\omega\hat{a}^\dagger\hat{a}t_F}\begin{pmatrix}\exp(-i\omega_a t_F/2) & 0\\ 0 & \exp(i\omega_a t_F/2)\end{pmatrix}. \tag{12}$$

The system evolution at the 'dressed' part of the cycle is described by

$$\hat{U}_D(t_D) = \exp\{-i[\omega\hat{a}^\dagger\hat{a} + (\omega - \Delta)\hat{\sigma}_3/2 + \Omega_0(\hat{\sigma}_+\hat{a} + \hat{a}^\dagger\hat{\sigma}_-)]t_D\}. \tag{13}$$

The later expression can be written in the matrix form as follows

$$\hat{U}_D(t_D) = \begin{pmatrix} e^{-i\omega_a t_D/2}(\cos\hat{\gamma}t_D - \frac{i\Delta}{2\hat{\gamma}}\sin\hat{\gamma}t_D) & -i\frac{\Omega_0\hat{a}}{\hat{\beta}}e^{-i\omega_a t_D/2}\sin\hat{\beta}t_D \\ -i\frac{\Omega_0\hat{a}^\dagger}{\hat{\gamma}}e^{i\omega_a t_D/2}\sin\hat{\gamma}t_D & e^{i\omega_a t_D/2}(\cos\hat{\beta}t_D + \frac{i\Delta}{2\hat{\beta}}\sin\hat{\beta}t_D) \end{pmatrix} \tag{14}$$

Here $\hat{\beta} = \sqrt{\Omega_0^2(\hat{a}^\dagger\hat{a}) + \Delta^2/4}$, $\hat{\gamma} = \sqrt{\Omega_0^2(\hat{a}^\dagger\hat{a}+1) + \Delta^2/4}$

The abrupt transition between the two stages allows to use the sudden approximation, i.e., to assume that the system's state remains unchanged during the switching. Thus the single-cycle evolution operator is

$$\hat{U}(T) = \hat{U}_F(t_F)\hat{U}_D(t_D). \tag{15}$$

The entangled field-atom state after K cycles of modulation is given by

$$|\psi(t = KT)\rangle = \hat{U}^K(T)|\psi(0)\rangle = [\hat{U}_F(t_F)\hat{U}_D(t_D)]^K|\psi(0)\rangle. \tag{16}$$

The field state projected by successful measurement of the atom in $|e\rangle$ after K cycles has the form, analogous to expressions (7-9), with φ_n:

$$\varphi_n = \arccos\left\{\cos(\beta_n t_D)\cos(\Delta t_F/2) - \frac{\Delta}{2\beta_n}\cos(\beta_n t_D)\cos(\Delta t_F/2)\right\} \tag{17}$$

It is possible to design more complicated modulation schemes, in which each cycle consist of *several unequal intervals with different detunings*. We can thereby control enough parameters to prepare a superposition of *several Fock states* with *arbitrary amplitudes* from an initial coherent state, by the same as described above. In Fig.6 we show that (a) superposition of 3 Fock states with *arbitrary pre-determined amplitudes* can be obtained from initial coherent states, using modulation with 3 different detunings and time intervals within each cycle; (b) The CM success probability is much *larger* than the squared project of the initial onto the final state.

This work has been supported by USARDSG, Minerva and the German–Israeli Foundation.

---

† Moscow Institute of Physics and Technology, Dolgoprudnii, Moscowskaja obl., Russia.

‡ The College of Staten Island, CUNY, 2800 Victory Boulevard, Staten Island, New York 10314

[1] J.H. Eberly, N.B. Narozhny and J.J. Sanchez-Mondragon, Phys. Rev. Lett. **44**, 1323 (1980).

[2] P.L. Knight and P.M. Radmore, Phys. Rev. A **26**, 676 (1982).

[3] E. Yablonovitch, Phys. Rev. Lett. **58**, 2059 (1987); J. Opt. Soc. Am. B **10**, 283 (1993).

[4] B. Sherman, G. Kurizki and A. Kadyshevitch, Phys. Rev. Lett. **69**, 1927 (1992); G. Kurizki, B. Sherman and A. Kadyshevitch, J. Opt. Soc. Am. B **10**, 346 (1993).

[5] Sinusoidal oscillations of the population inversion in the case of initial vacuum field have been recently analyzed for an atomic beam along a Fabry-Perot cavity axis, by G.M. Palma and F.S. Persico, Europhys.Lett. **17**, 207 (1992).

[6] J.P. Davis and P.J. Pechukas, J. Chem. Phys. **64** , 3129 (1976).

[7] A.B. Migdal and V.P. Krainov, *Approximation Methods in Quantum Mechanics*, (W. A. Benjamin 1969) p. 74 .
[8] A.M. Dykhne, Soviet Phys. JETP **11**, 411 (1960); Soviet Phys. JETP **14**, 941 (1962).
[9] B. Sherman and G. Kurizki, Phys. Rev. A **45**, R7674 (1992).
[10] J. Eiselt and H. Risken, Opt.Commun. **72**, 351 (1989).
[11] M. Brune, S. Haroche, J.M. Raimond, L. Davidovich and N. Zagury, Phys.Rev.A **45**, 5193 (1992).
[12] D. T. Pegg and S. M. Barnett, Phys. Rev. A **39**, 1665 (1989).
[13] Y. Yamamoto and H.A. Haus, Rev. Mod. Phys. **58**, 1001 (1986).
[14] S. Singh, Phys. Rev. A **25**, 3206 (1982).

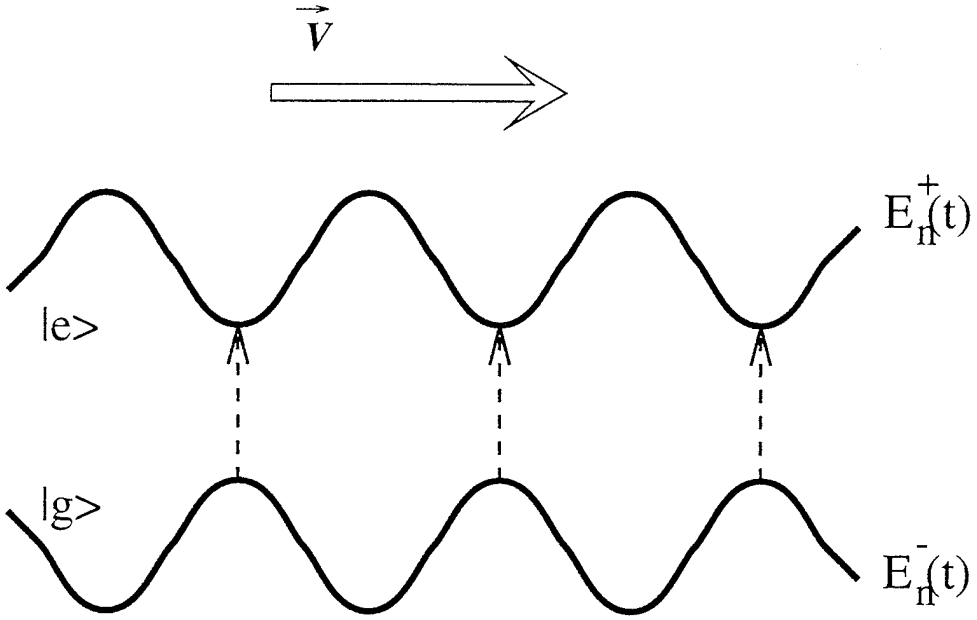

FIG. 1.

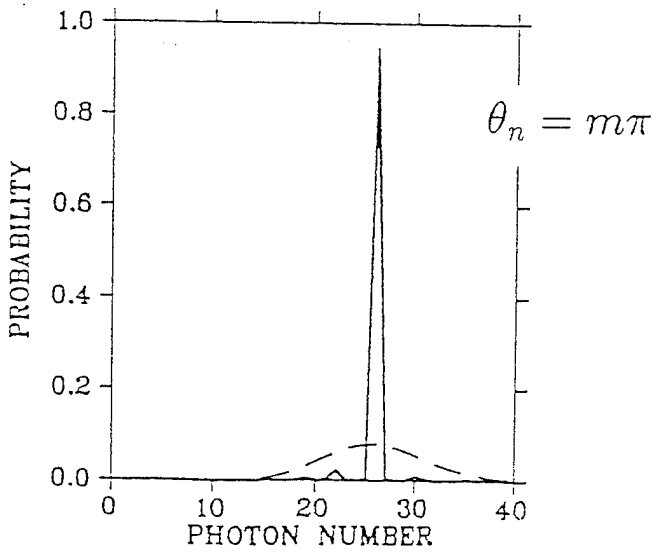

FIG. 2.

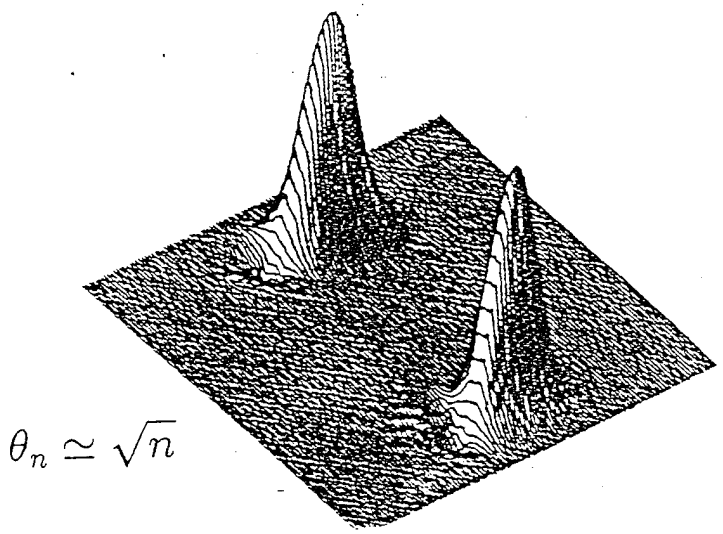
$\theta_n \simeq \sqrt{n}$

FIG. 3.

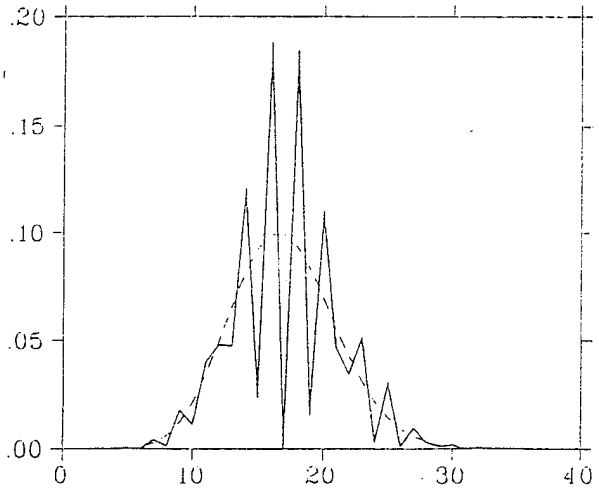
.20
.15
.10
.05
.00
0
10
20
30
40
$m\pi = \theta_{n_1}, \theta_{n_2}, \theta_{n_3}, \theta_{n_4}, \ldots$

FIG. 4.

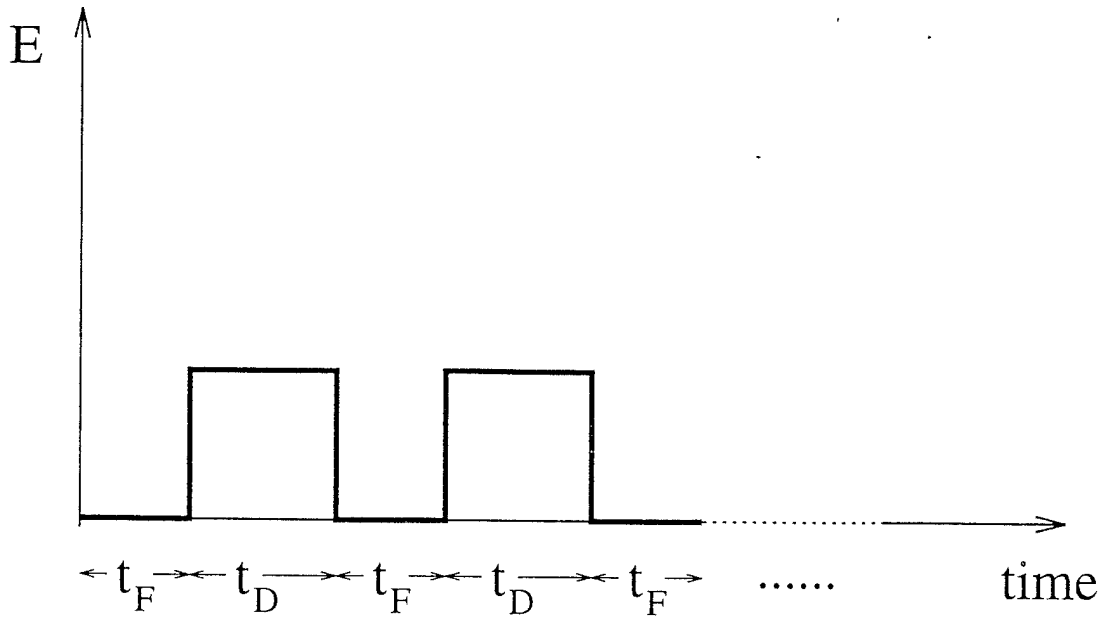
E
t_F
t_D
t_F
t_D
t_F
.....
time

FIG. 5.

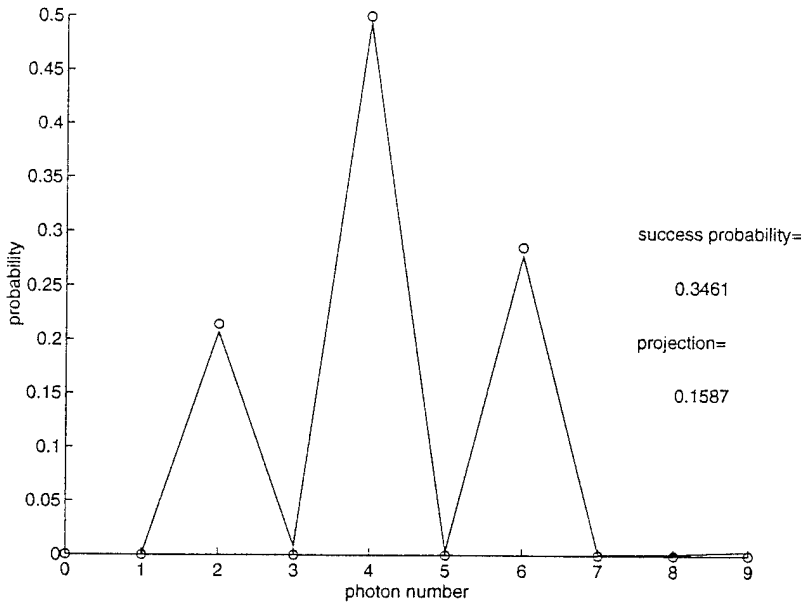
probability
photon number
success probability=
0.3461
projection=
0.1587

FIG. 6.

Appendix B:
Lasing Without Inversion via Spontaneously Formed Coherence in Photonic Band Gaps

A.G. Kofman and G. Kurizki

Chemical Physics Department, Weizmann Institute of Science, Rehovot 76100, Israel

Assume that the transition between a ground $|g\rangle$ and an excited $|e\rangle$ levels of the atom is near resonant to a photonic band. The strength of the atom-band coupling is characterized by the function

$$G(\omega) = \sum_{\lambda} |\kappa_\lambda|^2 \delta(\omega - \omega_\lambda), \tag{1}$$

where κ_λ is the matrix element of the coupling between the atom and the mode λ with the frequency ω_λ. The band is assumed to be well separated from other bands, so that the influence of the latter can be neglected. Moreover, the band is assumed to be sufficiently dense and narrow, i.e.,

$$G_m \gg \Delta_b, \ |\Delta_m|, \tag{2}$$

where G_m and Δ_b are the maximum value and the width of the function $G(\omega)$ respectively, $\Delta_m = \omega_a - \omega_m$, ω_m is the center of gravity of the band,

$$\omega_m = \frac{1}{A} \int_{\omega_U}^{\omega_L} d\omega \omega G(\omega), \tag{3}$$

ω_U and ω_L are the lower and upper band edges respectively, and

$$A = \int_{\omega_U}^{\omega_L} d\omega G(\omega). \tag{4}$$

Then the level e can be shown [1] to split to two levels 1 and 2, described by the normalized wavefunctions,

$$|\psi_j\rangle = \sqrt{c_j} \left[|e, 0_\lambda\rangle + \sum_{\lambda} \frac{\kappa_\lambda^*}{\omega_j - \omega_\lambda} |g, 1_\lambda\rangle \right] \quad (j = 1, 2). \tag{5}$$

The energies $\hbar\omega_{1,2}$ and the amplitudes $\sqrt{c_{1,2}}$ of the states 1 and 2 can be expressed through the moments of $G(\omega)$. In particular, the level separation to first approximation is

$$\omega_2 - \omega_1 = \sqrt{4A + \Delta_m^2} = \Omega_R, \tag{6}$$

where Ω_R is the vacuum Rabi frequency. An excited atom injected at $t = 0$ into the PBS in the case (2) undergoes an insignificantly small spontaneous decay over a time of order $1/\Omega_R$, after which the excited-state wavefunction becomes a *coherent superposition* of the states $|\psi_1\rangle$ and $|\psi_2\rangle$ [1],

$$|\Psi(t)\rangle = \sqrt{c_1} |\psi_1\rangle e^{-i\omega_1 t} + \sqrt{c_2} |\psi_2\rangle e^{-i\omega_2 t}, \tag{7}$$

If there is a nonzero matrix element of the dipole moment, d_{3e}, for the transition between the level e and another level 3, it then follows from (5) that the dipole moment matrix elements for the transitions 1-3 and 2-3 are given by

$$d_{31} = \sqrt{c_1} d_{3e}, \quad d_{32} = \sqrt{c_2} d_{3e}. \tag{8}$$

For the narrow-band, near-resonant case, $\Delta_m^2 \ll 4A$, which is of special interest here, one gets in the first approximation

$$c_1 = c_2 = \frac{1}{2}, \quad \omega_{1,2} = \frac{\omega_a + \omega_m}{2} \mp \sqrt{A}. \tag{9}$$

The density matrix elements of the system consisiting of the levels 1 and 2 are [cf. Eqs. (7) and (9)]

$$\rho_{11}(t) = \rho_{22}(t) = \frac{1}{2}, \quad \rho_{12}(t) = \rho_{21}^*(t) = \frac{\mathrm{e}^{2i\sqrt{A}t}}{2}. \tag{10}$$

The coherence between the levels 1 and 2 can be utilized to produce lasing without inversion [2]. Following Refs. [3–5], consider a Λ-system. The field

$$E(t) = E_0 \mathrm{e}^{-i\omega t} + \text{c.c.} \tag{11}$$

couples the upper level 3 with the lower levels 1 and 2. The levels 1, 2, and 3 have have the reciprocal lifetimes respectively γ_1, γ_2, and $\gamma_3 = \gamma_{31}' + \gamma_{32}' + \gamma_3'$, where γ_{31}', γ_{32}', and γ_3' are the spontaneous rates of transitions from the level 3 to the levels 1, 2, and all others respectively. The levels 1 and 2 can have finite lifetimes due to one or several of the following factors: spontaneous transitions to levels other than the ground state, finite time of presence of the atom in the structure, "background" of modes (outside the narrow band discussed above, which causes the splitting of level e), and collision-induced transitions. The open 3-level system consisting of the levels 1, 2, and 3 is described here by an unnormalized density matrix $R(t)$, whose diagonal elements yield the number of atoms in the laser cavity in the respective level. In the rotating wave approximation, the rotating-frame matrix elements of $R(t)$ obey the equations,

$$\begin{aligned}
\dot{R}_{11} &= -i(V_{13}R_{31} - V_{31}R_{13}) - \gamma_1 R_{11} + \gamma_{31}' R_{33} + W_{11}, \\
\dot{R}_{22} &= -i(V_{23}R_{32} - V_{32}R_{23}) - \gamma_2 R_{22} + \gamma_{32}' R_{33} + W_{22}, \\
\dot{R}_{33} &= -i(V_{31}R_{13} + V_{32}R_{23} - V_{13}R_{31} - V_{23}R_{32}) - \gamma_3 R_{33} + W_{33}, \\
\dot{R}_{12} &= (i\omega_{21} - \gamma_{21})R_{12} + i(V_{32}R_{13} - V_{13}R_{32}) + W_{12}, \\
\dot{R}_{13} &= (i\Delta_{31} - \gamma_{31})R_{13} + iV_{23}R_{12} - iV_{13}(R_{33} - R_{11}), \\
\dot{R}_{23} &= (i\Delta_{32} - \gamma_{32})R_{23} + iV_{13}R_{21} - iV_{23}(R_{33} - R_{22}).
\end{aligned} \tag{12}$$

Here $\Delta_{3j} = \omega_{3j} - \omega$, $V_{3j} = V_{j3}^* = -d_{3j}E_0/\hbar$ $(j = 1, 2)$, γ_{ij} is the decay rate of the nondiagonal matrix element R_{ij}, W_{33} is the pumping rate of atoms to level 3, $W_{ij} = q\rho_{ij}^0$ $(i, j = 1, 2)$, q being the rate at which atoms form a coherent superoisition of the states 1 and 2 (by spontaneous decay of $|e\rangle$), described by the normalized density matrix ρ_{ij}^0.

The complex susceptibility χ is expressed through the solution of Eqs. (12) by

$$\chi = \chi' - i\chi'' = \frac{4\pi}{VE_0^*}(d_{31}R_{13} + d_{32}R_{23}) \tag{13}$$

(in the Gaussian system of units), where V is the structure volume. The steady-state solution of Eqs. (12) yields in the first order in the field,

$$\chi = -\frac{4\pi i}{\hbar V}\left(\frac{|d_{13}|^2 N_{13} + f}{\gamma_{31} - i\Delta_{31}} + \frac{|d_{23}|^2 N_{23} + f^*}{\gamma_{32} - i\Delta_{32}}\right), \tag{14}$$

where $N_{i3} = R_{ii}^{(0)} - R_{33}^{(0)}$ $(i = 1, 2)$, $R_{ij}^{(0)}$ is the steady-state value of R_{ij} in the absence of the field,

$$R_{33}^{(0)} = \frac{W_{33}}{\gamma_3}, \quad R_{ii}^{(0)} = \frac{1}{\gamma_i}\left(W_{ii} + \frac{\gamma'_{3i}}{\gamma_3}W_{33}\right) \quad (i = 1, 2), \tag{15}$$

and

$$f = d_{31}d_{23}R_{12}^{(0)} = \frac{d_{31}d_{23}W_{12}}{\gamma_{21} - i\omega_{21}}. \tag{16}$$

Eqs. (13) and (14) yield

$$\chi'' = \frac{4\pi}{\hbar V}\mathrm{Re}\left(\frac{|d_{13}|^2 N_{13} + f}{\gamma_{31} - i\Delta_{31}} + \frac{|d_{23}|^2 N_{23} + f}{\gamma_{32} + i\Delta_{32}}\right). \tag{17}$$

The necessary condition for lasing is $\chi'' < 0$. Below we consider some situations where lasing is possible in the absence of inversion, i.e., for $N_{13} > 0$ and $N_{23} > 0$.

Let

$$\gamma_{31} = \gamma_{32} \tag{18}$$

and

$$\Delta_{31} = -\Delta_{32}, \quad \text{i.e.,} \quad \omega = (\omega_{31} + \omega_{32})/2. \tag{19}$$

Then for

$$\arg f = \pi - \phi, \quad \text{where} \quad \tan\phi = \frac{\omega_{21}}{2\gamma_{31}}, \tag{20}$$

the terms proportional to f in Eq. (17) are negative, yielding with the account of (16) and (17)

$$\chi'' = -\frac{4\pi}{\hbar V\sqrt{\gamma_{31}^2 + \omega_{21}^2/4}}\left[\frac{2|d_{31}d_{32}W_{12}|}{\sqrt{\gamma_{21}^2 + \omega_{21}^2}} - \frac{\gamma_{31}(|d_{31}|^2 N_{13} + |d_{32}|^2 N_{23})}{\sqrt{\gamma_{31}^2 + \omega_{21}^2/4}}\right]. \tag{21}$$

Consider first the case of a very small separation of the levels 1 and 2, $\omega_{21} \ll \gamma_{21}$, γ_{31}. In this case $\phi \approx \omega_{21}/(2\gamma_{31}) \ll 1$ in Eq. (20). Then

$$\chi'' = \frac{4\pi}{\hbar V \gamma_{31}} \left\{ -R_{33}^{(0)} \left[\left(1 - \frac{\gamma'_{31}}{\gamma_1} \right) |d_{31}|^2 + \left(1 - \frac{\gamma'_{32}}{\gamma_2} \right) |d_{32}|^2 \right] + \left[\frac{|d_{31}|^2 W_{11}}{\gamma_1} + \frac{|d_{32}|^2 W_{22}}{\gamma_2} - \frac{2|d_{31} d_{32} W_{12}|}{\gamma_{21}} \right] \right\}. \quad (22)$$

The second bracketed term here can be shown, with the help of inequalities $\gamma_{21} \geq (\gamma_1 + \gamma_2)/2$ and $\rho_{12}^0 \leq \sqrt{\rho_{11}^0 \rho_{22}^0}$, to be nonnegative. However, it can be made very small. In particular, it vanishes if

$$|\rho_{12}^0| = \rho_{11}^0 = \rho_{22}^0, \quad |d_{31}| = |d_{32}|, \quad (23)$$

$$\gamma_{12} = \gamma_1 = \gamma_2. \quad (24)$$

Then

$$\chi'' = -\frac{8\pi |d_{31}|^2 R_{33}^{(0)}}{\hbar V \gamma_{31}} \left(1 - \frac{\gamma'_{31} + \gamma'_{32}}{2\gamma_1} \right). \quad (25)$$

If $\gamma'_{31} + \gamma'_{32} < 2\gamma_1$ the lasing is possible for very small number of atoms at the levels 1 and 2, irrespective of the populations of the levels 1 and 2.

Consider now the opposite case of a large separation of the levels 1 and 2, $\omega_{21} \gg \gamma_{21}, 2\gamma_{31}$. In this case $\phi \approx \pi/2 - 2\gamma_{31}/\omega_{21} \approx \pi/2$ in Eq. (20). Assuming the validity of (23) which is justified in the above closely resonant case of the level splitting in a PBS [cf. (8)-(10)] and assuming also that

$$\gamma_1 = \gamma_2, \quad \gamma_{31} \approx \gamma_1/2, \quad (26)$$

Eq. (21) becomes

$$\chi'' = -\frac{16\pi \gamma_1 |d_{31}|^2}{\hbar V \omega_{21}^2} \left[R_{33}^{(0)} - \left(1 - \frac{\gamma_1}{2\gamma_{31}} \right) R_{11}^{(0)} \right]. \quad (27)$$

If $\gamma_{31} = (\gamma_1 + \gamma_3)/2$, the second inequality in (26) is equivalent to $\gamma_3 \ll \gamma_1$ and (27) becomes

$$\chi'' = -\frac{16\pi \gamma_1 |d_{31}|^2}{\hbar V \omega_{21}^2} \left(R_{33}^{(0)} - \frac{\gamma_3}{\gamma_1} R_{11}^{(0)} \right). \quad (28)$$

Equations (27) and (28) show that due to a coherent superposition of the states 1 and 2 only a very small fraction of the atoms in these states absorb the field $E(t)$ and therefore can yield gain when the number of the atoms at the level 3 is much less than the number of the atoms at the lower levels 1 and 2.

This work has been supported by USARDSG.

---

[1] A. G. Kofman, G. Kurizki, and B. Sherman, J. Mod. Opt. **41**, 353 (1994).
[2] M. O. Scully, S. Zhu, and A. Gavrielides, Phys. Rev. Lett. **62** , 2813 (1989).
[3] M. O. Scully, Phys. Rev. Lett. **67**, 1855 (1991).
[4] N. Lu, Phys. Rev. A **45**, 5011 (1992).
[5] U. Rathe *et al.*, Phys. Rev. A **47**, 4994 (1993).

Appendix C:
Photon Exchange by Atom Pairs in Resonators

G. Kurizki, A. G. Kofman
Chemical Physics Department, Weizmann Institute of Science, Rehovot 76100, Israel

V. Yudson
Physics Dept., University of Ulm, 89069 Ulm, Germany.

(June 13, 1995)

A system of two identical atoms sharing a photon with a high-Q resonator mode is studied by a non-perturbative formalism. As opposed to previously considered models, here the interatom coupling is shown to result from competing effects of vacuum Rabi splitting and photon exchange via off-resonant modes. Strong suppression of interatom excitation transfer is predicted at both near- and far-zone separations.

PACS numbers: 42.50.Fx, 42.50.Md

The physical importance of a system of two resonant atoms sharing a photon is evident from the numerous studies of its various aspects: causality and retardation of the interatomic photon exchange [1]; atomic level shifts due to the photon exchange, which are identical with the resonant dipole-dipole interaction (RDDI) [2,3]; oscillatory cooperative decay in diatom dissociation [4]; spectra [5] and squeezing [6] of two-atom resonance fluorescence. The above literature has dealt with atoms in open space, whereas studies of cooperative atomic effects in resonant cavities have been extensions of the Tavis-Cummings model [7]. This model assumes many atoms identically coupled to a single mode and ignores the symmetry-breaking dipole-dipole effects, which are important at near-zone separations [3,5].

This Rapid Communication is aimed at gaining new insight into systems which are now becoming experimentally realizable [8]: a pair of identical two-level atoms (or excitons), sharing a photon with one or many high-Q modes in a resonator. To this end, we develop a formalism capable of treating two atoms coupled to a field with an *arbitrary* mode-density spectrum in *a non-perturbative fashion.* Such a formalism is necessary because the standard perturbative treatment of two-atom coupling, to second order in the field [2], is *inadequate* for a reservoir whose mode-density spectrum does not vary smoothly, as demonstrated already by our comprehensive theory of a single atom coupled to such a reservoir [9]. We predict drastic modifications (as compared to previously studied models) of the energy levels and interatom excitation transfer in such systems, both at near-zone and far-zone atomic separations. These modifications are due to *interfering* (competing) effects of strong atomic coupling to high-Q modes (vacuum Rabi splitting [7]) and interatom photon exchange via all other modes (RDDI [2,3]).

Here we concentrate [10] on a system of atoms A and B that are nearly-resonant with a cavity mode or band of degenerate modes (as in spherical resonators). The effective Hamiltonian, which can be derived from first principles, has then the following second-quantized form in the rotating-wave approximation (RWA)

$$H = \hbar(\omega_A|e_A\rangle\langle e_A| + \omega_B|e_B\rangle\langle e_B|)$$

$$+ \hbar M(|e_A\rangle\langle e_B| + |e_B\rangle\langle e_A|) + \hbar \sum_\lambda \omega_\lambda a_\lambda^\dagger a_\lambda$$
$$+ \hbar \sum_\lambda (\kappa_{A\lambda} a_\lambda |e_A\rangle\langle g_A| + \kappa_{B\lambda} a_\lambda |e_B\rangle\langle g_B| + \text{H.c.}). \quad (1)$$

Here $|e_{A(B)}\rangle$ and $|g_{A(B)}\rangle$ are the excited and ground atomic states. The frequency ω_λ and annihilation operator a_λ pertain to a near-resonant field mode labeled by λ whose position-dependent dipolar coupling to atom A or B is given by $\kappa_{A(B)}$; $\hbar\omega_{A(B)}$ are the excited-state energies including the spatially-dependent shifts due to single-atom interactions with the field reservoir *outside* the near-resonant narrow line (band) and M is the matrix element of the interatom interaction via the same reservoir calculated by second-order perturbation theory [2,3]. Both $\hbar\omega_{A(B)}$ and M may have imaginary parts (see below).

The time-dependent wavefunction for the system of a single photon shared by the field and atoms can be written as

$$|\Psi_b(t)\rangle = \alpha_{Ab}(t)|e_A g_B, \{0_\lambda\}\rangle + \alpha_{Bb}(t)|e_B g_A, \{0_\lambda\}\rangle$$
$$+ \sum_\lambda \beta_{\lambda b}(t)|g_A g_B, 1_\lambda\rangle, \quad (2)$$

where $|\{0_\lambda\}\rangle$ and $|1_\lambda\rangle$ are the vacuum and λ-mode single-photon states, respectively, whereas $b = A, B$ denotes which atom is excited initially. The Schrödinger equation yields the following *exact* Laplace-transform solutions (within the RWA) for the excited-state S-matrix

$$\hat{\alpha}(s) = D^{-1}(s)\hat{U}(s). \quad (3)$$

Here $\hat{\alpha}(s)$ and $\hat{U}(s)$ are 2×2 matrices in the basis of $|e_{A(B)}g_{B(A)}\rangle$. The diagonal elements of $\hat{U}(s)$ are $U_{AA(BB)} = s + i\omega_{B(A)} + iJ_{B(A)}(s)$, where

$$J_{A(B)}(s) = \int \frac{G_{A(B)}(\omega)d\omega}{is - \omega},$$
$$G_{A(B)}(\omega) = \sum_\lambda |\kappa_{A(B)\lambda}|^2 \delta(\omega - \omega_\lambda). \quad (4)$$

Here and henceforth the integration is performed only over the narrow band of near-resonant modes. The off-diagonal elements are $U_{AB(BA)}(s) = -iM - iJ_{AB(BA)}(s)$, where

$$J_{AB(BA)}(s) = \int \frac{G_{AB(BA)}(\omega)d\omega}{is - \omega},$$
$$G_{AB(BA)}(\omega) = \sum_\lambda \kappa_{A(B)\lambda}\kappa^*_{B(A)\lambda}\delta(\omega - \omega_\lambda). \quad (5)$$

The resolvent (denominator) of Eq. (3), $D(s)$, is the determinant of the matrix $\hat{U}(s)$. The roots of the equation $D(s) = 0$, which correspond to the levels (eigenvalues) of the system, can differ strongly from the standard perturbative solutions, as shown below. Our subsequent analysis rests on the following assumptions. (i) The transition frequencies and decay rates of atoms A and B are equal, which is true for identical atoms far from cavity walls or dielectric-layer interfaces. (ii) The transition dipole moments are real and the mode functions are standing waves, i.e., also real; then $G_{AB}(\omega) = G_{BA}(\omega)$ is real, yielding $U_{AB}(s) = U_{BA}(s)$, whence $\alpha_{AB}(t) = \alpha_{BA}(t)$.

The case of weak atom-reservoir coupling obtains if the near-resonant line (band) is sufficiently broad and not sharp (e.g, a single mode broadened due to its finite Q-factor). By suitable extension of the validity conditions for the Weisskopf-Wigner approximation for single-atom emission [9], we find that this case holds if the mode-density spectrum is smooth enough, so that

$$\left|\frac{dJ_{A(B)}}{d\omega_A}\right| \ll 1, \quad \left|\frac{dG_{A(B)}(\omega_A)}{d\omega}\right| \ll \frac{G_{A(B)}(\omega_A)}{|\mathrm{Re}J_{A(B)}|}, \tag{6}$$

where $J_{A(B)} = J_{A(B)}(-i\omega_A + 0)$. We then replace the near-resonant contributions $J_{A(B)}(s)$ and $J_{AB}(s)$ by constants, $J_{A(B)}$ and $J_{AB} = J_{AB}(-i\omega_A + 0)$ respectively [see Eqs. (4) and (5)], and absorb them into the single-atom and two-atom level shifts and the respective decay rates. The resulting eigenvalues and eigenstates of the singly-excited system are then

$$\begin{aligned} \omega_{s(a)} &= \mathrm{Re}\tilde{\omega}_A \pm \mathrm{Re}\tilde{M}, \\ |\psi_{s(a)}\rangle|\{0_\lambda\}\rangle &= \frac{1}{\sqrt{2}}(|e_A g_B\rangle \pm |g_A e_B\rangle)|\{0_\lambda\}\rangle, \end{aligned} \tag{7}$$

where $\tilde{\omega}_{A(B)} = \omega_{A(B)} + J_{A(B)}$, $\tilde{M} = M + J_{AB}$, and s (a) denotes the symmetric (antisymmetric) eigenstates. These two states are split by the RDDI shift (which is modified by the structure) and give rise to damped sinusoidal oscillations of the excitation-transfer probability from A to B at a rate of $2\mathrm{Re}\tilde{M}$, which varies as R^{-3} at near-zone separations, $\omega_A R/c \ll 1$ [2,3].

We shall be primarily concerned with the very different behavior obtained in the case of a sharp, narrow line or band whose center of gravity is at ω_0. Consistently, one can use in Eqs. (4) and (5) the approximation $G_{A(B)}(\omega) \approx N\kappa^2_{A(B)0}\delta(\omega - \omega_0)$ and $G_{AB}(\omega) \approx \sum_\lambda \kappa_{A\lambda}\kappa^*_{B\lambda}\delta(\omega - \omega_0)$, N being the number of near-resonant modes in the narrow band and $|\kappa_{A(B)0}|$ the root-mean-square of $|\kappa_{A(B)\lambda}|$. This approximation holds if $\sqrt{N}|\kappa_{A(B)0}|$ is much greater than the band width. It implies that we neglect *all dissipation*, i.e., the decay rates $\tilde{\gamma}_A$ and $\mathrm{Im}M$, originating from the background density of modes outside the line (band), since they are assumed to be much smaller than the oscillation frequencies in the system, and we are interested in times $\ll \tilde{\gamma}_A^{-1}$, $|\mathrm{Im}M|^{-1}$. As a second simplification, we shall confine ourselves to the case $\sum_\lambda \kappa_{A\lambda}\kappa^*_{B\lambda} = N\kappa_{A0}\kappa_{B0}$, which holds for a single near-resonant mode or a fully degenerate mode, such that $\kappa_{A\lambda}/\kappa_{B\lambda}$ is independent of λ (otherwise, $|\sum_\lambda \kappa_{A\lambda}\kappa^*_{B\lambda}| < N|\kappa_{A0}\kappa_{B0}|$). We shall take $\kappa_{A0} > 0$ and the sign of κ_{B0} to be that of the ratio $\kappa_{A\lambda}/\kappa_{B\lambda}$. Following these two simplifications, the equation $D(s = -i\omega) = 0$ becomes

$$\begin{aligned} -\left(\omega - \omega_A - \frac{N\kappa^2_{A0}}{\omega - \omega_0}\right)\left(\omega - \omega_B - \frac{N\kappa^2_{B0}}{\omega - \omega_0}\right) \\ + \left(M + \frac{N\kappa_{A0}\kappa_{B0}}{\omega - \omega_0}\right)^2 = 0. \end{aligned} \tag{8}$$

We have now reduced the problem to that of two atoms coupled to a single mode via coupling constants $\sqrt{N}\kappa_{A0}$ and $\sqrt{N}\kappa_{B0}$, and to each other via matrix element M. A Hamiltonian describing this problem can be written as a 3×3 matrix in the basis of the states $|e_{A(B)}g_{B(A)}, \{0\}\rangle$ and $|g_A g_B, 1_0\rangle$, where 0 and 1_0 are the vacuum and single-photon numbers in the near-resonant mode. We have evaluated in closed form the eigenvalues (Fig. 1) and

eigenfunctions corresponding to Eq. (8), yet it will be more illustrative to focus on the following distinct limits:

(a) Let us assume that $\kappa_{A0} \approx \kappa_{B0}$. This approximate equality of the atomic couplings to the mode holds for identical atoms with parallel dipoles *in the near zone of separations*, $\omega_A R/c \ll 1$. In this approximation the eigenvalues are given by

$$\omega_3 \approx \omega_a, \quad \omega_{1,2} \approx \omega_\pm = \frac{1}{2}(\omega_s + \omega_0 \pm \Omega);$$
$$\Omega = \sqrt{2N(\kappa_{A0} + \kappa_{B0})^2 + (\omega_s - \omega_0)^2}, \tag{9}$$

where now $\omega_{s(a)} = (\omega_A + \omega_B)/2 \pm M$. These results hold over most of the near-zone separation interval (except for the range specified below). For $|\omega_s - \omega_0| \gg \sqrt{2N}(\kappa_{A0} + \kappa_{B0})$, which is the case, e.g., for $R \to 0$, Eq. (9) yields that ω_+ and ω_- tend to ω_s and ω_0, indicating that the near-resonant field mode is decoupled from the RDDI-split symmetric and antisymmetric states. Throuhout the range of validity of Eq. (9), only the antisymmetric-state eigenvalue remains unperturbed, since the coupling of this state to the mode $2^{-1/2}(\kappa_{A0} - \kappa_{B0}) \approx 0$ in the near zone. By contrast, the symmetric state and the single-photon state become hybridized, giving rise to two eigenvalues that are split by $\pm\Omega$, the symmetric-state vacuum Rabi frequency. The above trends are also reflected by the corresponding dressed-state eigenfunctions

$$|\psi_3\rangle \approx |\psi_a, \{0\}\rangle, \quad |\psi_{1,2}\rangle \approx |\psi_\pm\rangle$$
$$= \sqrt{c_\pm}\left[|\psi_s, \{0\}\rangle \pm \sqrt{2N}\frac{\kappa_{A0} + \kappa_{B0}}{\Omega \pm (\omega_s - \omega_0)}|g_A g_B, 1_0\rangle\right], \tag{10}$$

where $c_\pm = [1 \pm (\omega_s - \omega_0)/\Omega]/2$. We note that $|\psi_s, \{0\}\rangle$ and $|g_A g_B, 1_0\rangle$ coincide with $|\psi_+\rangle$ and $|\psi_-\rangle$ for $|\omega_s - \omega_0| \gg \sqrt{2N}(\kappa_{A0} + \kappa_{B0})$, but otherwise the symmetric and single-photon states are strongly mixed in $|\psi_\pm\rangle$.

These eigenfunctions can be used to calculate the probability of excitation transfer, say, from the initially excited atom A to the initially unexcited atom B, $P_B(t)$, and the corresponding excitation-trapping probability $P_A(t)$,

$$P_{B(A)}(t) = \left|\sum_{i=1}^{3}\langle\psi_{B(A)}|\psi_i\rangle\langle\psi_i|\psi_A\rangle e^{-i\omega_i t}\right|^2, \tag{11}$$

where $|\psi_{A(B)}\rangle = |e_{A(B)}g_{B(A)}, \{0\}\rangle$. Thus, the two-atom symmetry determines the Rabi splitting, whence we find *three* distinct atomic-state frequencies, causing aperiodic oscillations of $P_{B(A)}(t)$, instead of sinusoidal oscillations in previously studied cases [2,7]. The time averaged probabilities, $\bar{P}_{B(A)} = \sum_{i=1}^{3}\left|\langle\psi_{B(A)}|\psi_i\rangle\langle\psi_i|\psi_A\rangle\right|^2$, are approximately equal, $\bar{P}_A \approx \bar{P}_B$, varying from 3/8 at $|\omega_s - \omega_0| \ll \sqrt{2N}(\kappa_{A0} + \kappa_{B0})$ to the free space value 1/2 at $|\omega_s - \omega_0| \gg \sqrt{2N}(\kappa_{A0} + \kappa_{B0})$ (note that in this system $P_A(t) + P_B(t) < 1$, because of the nonzero probability of the mode excitation).

(b) Let us now consider the effect of the small near-zone difference $\kappa_{A0} - \kappa_{B0}$ which scales approximately linearly with the separation R. This effect is most remarkable in the range of separations, corresponding to *pseudocrossing* (near-equality) of two eigenvalue curves in Eq. (9) (solid curves on Fig. 1), $\omega_+ \approx \omega_3$ for $M < 0$ and $\omega_- \approx \omega_3$ for $M > 0$. We shall

assume below that M is positive in the near zone. The pseudocrossing separation R_c can be estimated from Eq. (9) for the parameters that maximize $\kappa_{A(B)0}$: a single mode confined to the smallest possible volume $\sim \lambda_A^3$ (where $\lambda_A = 2\pi c/\omega_A$), transition dipole moment $d_A \sim ea$, a being the excited state radius, and, corresppondingly, $\omega_A \sim e^2/(\hbar a)$. Using the maximal estimate for RDDI, $M \sim (ea)^2/R^3$, this yields (i) $R_c \sim N^{-1/6}\sqrt{\alpha/(2\pi)}\lambda_A$, where $\alpha = 1/137$, if $|\omega_0 - \omega_A| \lesssim \sqrt{2N}(\kappa_{A0}+\kappa_{B0})$; (ii) $R_c \sim [\omega_0 - \omega_A/(N\omega_A)]^{1/3}\lambda_A$, if $\omega_0 - \omega_A \gg \sqrt{2N}(\kappa_{A0}+\kappa_{B0})$. In either case, $R_c \ll \lambda_A$, i.e., the pseudocrossing occurs *well within the near zone*. Note that for certain dipole orientations M is further reduced and R_c can become even smaller.

Drastic modifications of the interatomic coupling occur near R_c (as compared to the cases discussed above), due to the strong competition of RDDI and Rabi splittings. The eigenvalues in Eq. (9) are then replaced by the more accurate solutions of Eq. (8)

$$\omega_1 \approx \omega_+, \quad \omega_{2,3} \approx \frac{1}{2}(\omega_- + \omega_a \pm \Omega'),$$
$$\Omega' = \sqrt{V_0^2 + (\omega_- - \omega_a)^2}, \quad V_0 = \frac{N(\kappa_{A0}^2 - \kappa_{B0}^2)}{\sqrt{\Omega(\Omega + \omega_0 - \omega_s)}}. \tag{12}$$

Here $|V_0|$ equals the minimal splitting $\omega_2 - \omega_3$ and also determines the width of the pseudocrossing interval, which is defined as follows: $\Delta R_c = |R_1 - R_2|$, where $\omega_{a-}(R_{1,2}) = |V_0|$ and $\omega_{a-} = |\omega_a - \omega_-|$. For two atoms far from a node of a sinusoidal mode, $V_0 \sim N\kappa_{A0}|\kappa_{A0} - \kappa_{B0}|/(\sqrt{8N}\kappa_{A0} + |\omega_0 - \omega_s|)$ and is proportional to R_c at near-zone separations [11].

The eigenfunction $|\psi_+\rangle$ is not affected by the pseudocrossing, whereas $|\psi_-\rangle$ and $|\psi_a\rangle$ are strongly mixed near R_c, forming

$$|\psi_{2,3}\rangle = \sqrt{b_{2,3}}\left[|\psi_-\rangle \pm \frac{V_0}{\Omega' \pm (\omega_- - \omega_a)}|\psi_a, \{0\}\rangle\right], \tag{13}$$

where $b_{2,3} = [1 \pm (\omega_- - \omega_a)/\Omega']/2$. This mixing implies the complete breaking of the symmetry [Eq. (7)], which characterizes the two-atom system subject to RDDI in the weak-coupling case. At $R = R_c$, $|\psi_{2,3}\rangle = 2^{-1/2}(|\psi_-\rangle \pm |\psi_a, \{0\}\rangle)$. For sufficiently large and positive detuning $\omega_0 - \omega_s \approx \Omega$, $c_+ \to 0$, yielding [see Eq. (10)] $|\psi_2\rangle \to |e_A g_B, \{0\}\rangle$, and $|\psi_3\rangle \to |e_B g_A, \{0\}\rangle$, which means that the excited states of atoms A and B become *uncoupled*, due to interference of $|\psi_s\rangle$ and $|\psi_a\rangle$. The corresponding time-averaged value of the excitation transfer probability exhibits *strong suppression* in the pseudocrossing interval, $\bar{P}_B(R = R_c) = 3c_+^2/8 \ll 1$. Concurrently, $\bar{P}_A(R = R_c) = 1 - c_+ + (3/8)c_+^2$, tending to 1 with the increase of $\omega_0 - \omega_s$ (solid curves in Fig. 2). This means that *the excitation is then strongly trapped at the initial atom*, which reflects the decoupling of the atomic excited states. These results sharply contrast those outside the crossing region [limit (a) above].

(c) Finally, let us examine the limit of large differences between the couplings: $\kappa_a \equiv 2^{-1/2}|\kappa_{A0} - \kappa_{B0}| \sim \kappa_s \equiv 2^{-1/2}|\kappa_{A0} + \kappa_{B0}|$. For atoms with non-parallel dipoles, this limit can occur at any separation. The analysis of Eq. (8) in this limit shows that the results of limit (b) apply to the pseudocrossing of ω_a with ω_-, if $\omega_0 - \omega_A \gg \kappa_{s(a)}$. The only salient difference with limit (b) is in the *width* of the pseudocrossing region. According to the discussion following Eq. (12) this region is defined by $\omega_{a-}(R) \equiv |\omega_a(R) - \omega_-(R)| \lesssim |V_0(R)|$. Under the condition $\omega_0 - \omega_A \gg \kappa_s \sim \kappa_a$, we find that $\omega_{a-}(R)$ increases with R for $R > R_c$,

until it attains its upper bound $N\kappa_s^2/(\omega_0 - \omega_A)$. On the other hand, $|V_0|$ decreases for $R > R_c$ down to its lower bound $N\kappa_s\kappa_a/(\omega_0 - \omega_A)$ (actually this bound is slowly varying due to the spatial dependence of $\kappa_{s,a}$, but this does not change $|V_0|$ appreciably). Since these two bounds coincide, the pseudocrossing region can extend from $R \lesssim R_c \ll \lambda_A$ to $R \gg \lambda_A$ (dashed curves in Fig. 1) (!). Throughout this region, Eqs. (12) and (13) hold fully, i.e., excitation transfer is *strongly suppressed* by interference of $|\psi_s\rangle$ and $|\psi_a\rangle$ (dashed curves in Fig. 2). Similar results hold also for $\omega_A - \omega_0 \gg \kappa_{s(a)}$.

The analytical treatment outlined above is in full agreement with the numerical analysis of the exact Eq. (3) (as shown in Figs. 1 and 2). Both treatments demonstrate that two identical atoms interacting via a near-resonant narrow-linewidth mode (or degenerate band) and an off-resonant reservoir can exhibit a much richer variety of spectral and dynamical features than what is currently known. It must be viewed as a system of *three* mutually coupled excited states (as opposed to *two* such states in previously studied models [2,7]). The dipole-dipole (RDDI) coupling and the mode-induced Rabi splitting are *inseparable* in this system. The interatom coupling results from mixing of all three states, which is most striking for separations where the two predominantly-populated levels nearly cross. Then the competing RDDI and Rabi splittings cause strong interference of the symmetric and antisymmetric two-atom excited states, leading to *decoupling* of single-atom excited states. This occurs at near-zone (quasimolecular) separations (as small as $10^{-2}\lambda_A$) and corresponds to *suppression* of interatom excitation transfer, compared to the electrostatic near-zone limit of RDDI.

The present predictions, particularly the suppression of excitation transfer at quasimolecular separations, may be important in various systems of two atoms, molecules, or excitons within high-Q resonators. Dielectric sphere surfaces and Bragg resonators are particularly suitable configurations. Control of the initial state of each partner, even at short separations, can be achieved by: (i) excitation of only one partner, say A, to $|e_A\rangle$, via another state $|u_A\rangle$ which *differs* from its counterpart in B, although the transitions $|e_A\rangle \to |g_A\rangle$ and $|e_B\rangle \to |g_B\rangle$ are identical (this option is common in molecules or impurity-bound excitons); (ii) single-partner excitation localized on a 10^2 nm scale (by electronic, XUV or near-field optical techniques); (iii) slow (ultracold) atom collisions in a cavity, with one atom initially excited outside the cavity. The dipole orientations are controllable by the initial excitation and (or) by magnetic splitting of Zeeman sublevels.

This work has been supported by USAR DSG and the Minerva Foundation, Germany.

---

[1] E. Fermi, Rev. Mod. Phys. **4**, 87 (1932); J. Hamilton, Proc. R. Soc. A **63**, 12 (1949); P. W. Milonni and P. L. Knight, Phys. Rev. A **10**, 1096 (1974).

[2] D. P. Craig and T. Thirunamachandran, *Molecular Quantum Electrodynamics* (Academic, London, 1984).

[3] G. S. Agarwal, *Quantum Statistical Theories of Spontaneous Emission* (Springer, Berlin, 1974).

[4] Kurizki and A. Ben-Reuven, Phys. Rev. A **32**, 2560 (1985); A **36**, 90 (1987); P. Grangier, A. Aspect and J. Vigue, Phys. Rev. Lett. **54**, 418 (1985).

[5] H. Freedhof, Phys. Rev. A **19**, 1132 (1979); Y. Ben-Aryeh and C.M. Bowden, IEEE J. Quantum Electron. **24**, 1376 (1988); G. V. Varada and G. S. Agarwal, Phys. Rev. A **45**, 6721 (1992).

[6] G. Kurizki, Phys. Rev. A **43**, 2599 (1991).

[7] M. Tavis and F. W. Cummings, Phys. Rev. **188**, 692 (1969); G. S. Agarwal, Phys. Rev. Lett. **53**, 1732 (1984); M. G. Raizen et al., Phys. Rev. Lett. **63**, 240 (1989).

[8] F. DeMartini et al., Phys. Rev. Lett. **65**, 1853 (1990); Y. Yamamoto et al., Opt. and Quant. Elec. **24S**, 215 (1992).

[9] A. G. Kofman, G. Kurizki, and B. Sherman, J. Mod. Opt. **41**, 353 (1994).

[10] Application of this formalism to two atoms with resonance frequency in a photonic band gap (near the band edge) will be treated elsewhere.

[11] Generally, $\omega_A - \omega_B$ should be added to the above expression for V_0. However for identical atoms far from cavity walls $|\omega_A - \omega_B| \sim [(ea)^2/\lambda_A^3](\omega_A R_c/c) \ll V_0$.

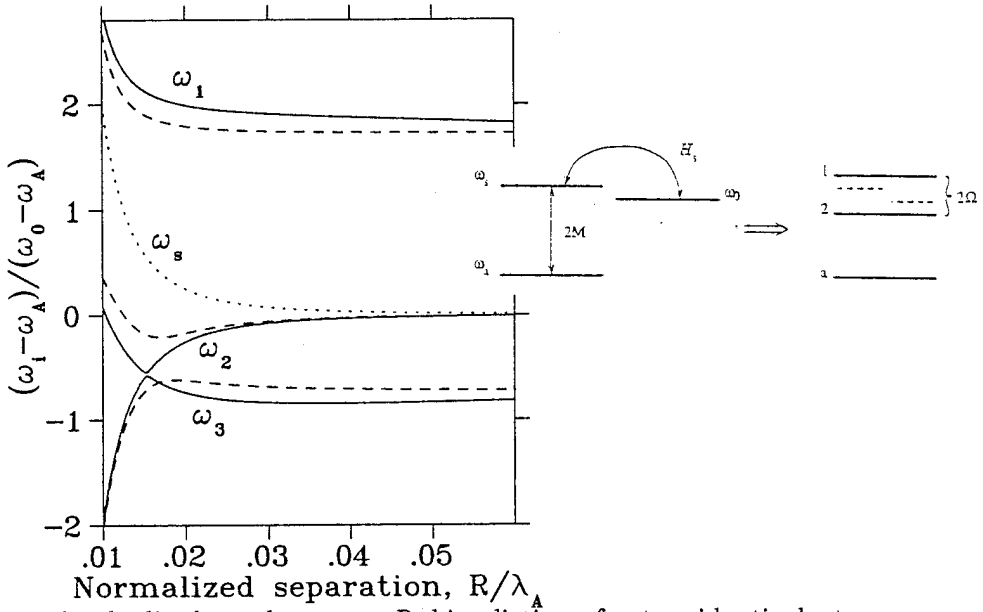

FIG. 1. Inset – competing dipole-dipole and vacuum Rabi splittings for two identical atoms coupled to a near-resonant mode. Solid curves – exact eigenvalues as a function of the normalized separation R/λ_A for $N = 1$, $M = (\gamma_A/2)(\omega_A R/c)^{-3}$, where γ_A is the free space decay rate of the atom excited state, $\omega_0 - \omega_A = 10^3\gamma_A$, $\kappa_{A(B)} = 10^3\gamma_A \sin(\omega_A r_{A(B)}/c)$, and $r_A = 0.3\lambda_A$. Note the narrow pseudocrossing region. Dashed curves – idem, for $\kappa_A = 1000\gamma_A$ and $\kappa_B = 500\gamma_A$. The pseudocrossing region is now very broad.

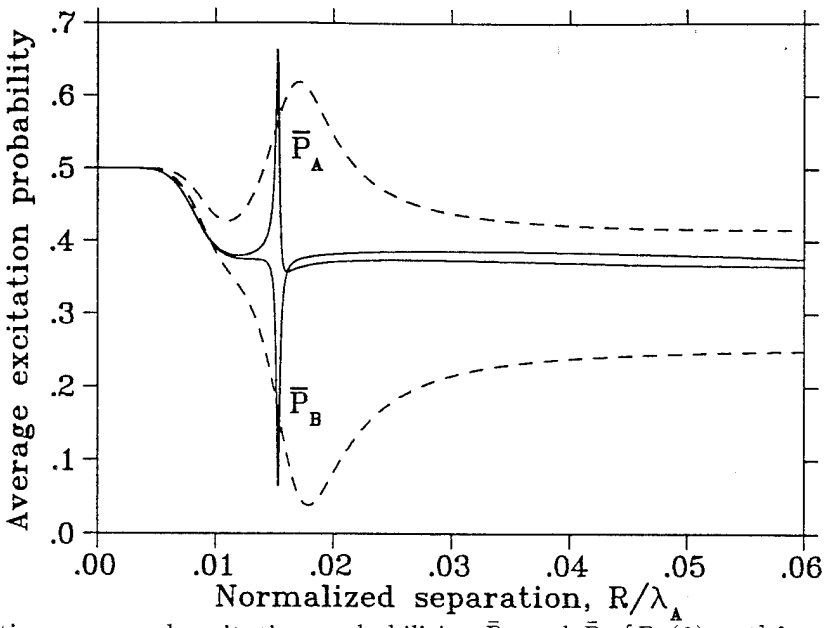

FIG. 2. The time-averaged excitation probabilities $\bar{P}_A$ and $\bar{P}_B$ $[P_A(0) = 1]$ for same parameters as in Fig. 1: solid curves – for narrow interval of excitation-transfer suppression; dashed curves – for broad interval of suppression.

Appendix D:
Self-Induced Transparency in Bragg Reflectors: Gap Solitons Near Absorption Resonances

Alexander Kozhekin and Gershon Kurizki
Chemical Physics Department, Weizmann Institute of Science, Rehovot 76100, Israel

We show that pulse transmission through near-resonant media embedded within periodic dielectric structures can produce self-induced transparency (SIT) in the band gap of such structures. This SIT constitutes a principally new type of gap soliton.

42.50Rh, 42.25.Bs, 03.40.Kf, 78.66.-w.

Self-induced transparency (SIT), namely, solitary propagation of electromagnetic (EM) pulse in near-resonant media, irrespective of the carrier-frequency detuning from resonance, is one of the most striking and important effects of nonlinear optics [1,2]. It reflects the essence of driven two-level atom dynamics, which is described, in the soliton frame, by a pendulum equation for the pulse area θ (the sine-Gordon equation). If the pulse duration is much shorter than the transition (spontaneous-decay) lifetime (T_1) and dephasing time (T_2), and θ is a multiple of 2π, then pulse-area conservation gives rise to SIT, corresponding to re-emission of the absorbed radiation in-phase with the driving field.

One of the standard tacit requirements for SIT is uniformity of the medium. Indeed, one would expect that partial reflection of the field in a non-uniform, e.g., layered, medium should destroy SIT, because the pulse area is then split between the forward and backward (reflected) waves, and is no longer conserved for each wave. This expectation seems to be supported by treatments of a single thin resonant film [3] or periodic array of such films [4], which yield bistable (two-valued) transmission of the incident pulse, owing to the coupling of the forward and backward waves. Should we then anticipate severely hampered transmission through a medium whose resonance lies in a reflective spectral domain (photonic band gap) of a periodically-layered structure (a Bragg reflector)? In this Letter we show that, contrary to such expectations, it is possible for the pulse to overcome the band-gap reflection and produce SIT in a near-resonant medium embedded in a Bragg reflector.

The predicted SIT propagation is a principally new type of gap soliton, which does not obey any of the familiar soliton equations, such as the non-linear Schrödinger equation (NLSE) or the sine-Gordon equation. Its spatio-temporal form, intensity dependence and transmission mechanism are shown here to be quite unique. Nevertheless, it shares several common features with the extensively - studied gap solitons [5–8] or with ultrashort pulses [9] in Kerr-nonlinear Bragg reflectors.

We consider the propagation of an EM pulse through a medium consisting of two-level systems (TLS) embedded within a one-dimensional periodic dielectric structure, e.g., a multi-layered dielectric mirror. Our starting point is the Maxwell equation for the field E

$$c^2\frac{\partial^2 E}{\partial z^2}-\frac{\partial^2 E}{\partial t^2}=\frac{\partial^2 P_{\rm tot}}{\partial t^2} \tag{1}$$

driven by the current of the total polarization $P_{\rm tot}=P_{\rm lin}+P_{\rm nl}$. The linear part of the polarization $P_{\rm lin}=\chi_{\rm lin}E$ is characterized by a linear refractive index $n_{\rm lin}=\epsilon_{\rm lin}^{1/2}=(1+$

$4\pi\chi_{\rm lin})^{1/2}$ with fundamental period d, $\epsilon_{\rm lin} = \epsilon_0 + \sum_{m=1}^{\infty} \Delta\epsilon_m \cos(2mkz)$, where $k = \pi/d$ and $\Delta\epsilon_m$ is the variation of m-th harmonic of the dielectric index. The non-linear polarization $P_{\rm nl}$ is the near-resonant response of the TLS.

We may, analogously to the theory of distributed feedback lasers [10–12], decompose the total field and non-linear polarization into forward (F) and back-reflected (B) components

$$E(z,t) = \left[\mathcal{E}_F(z,t)e^{ikz} + \mathcal{E}_B(z,t)e^{-ikz}\right] e^{-i\omega_{gc}t} + \text{c.c} \tag{2a}$$

$$P_{\rm nl}(z,t) = \left[\mathcal{P}_F(z,t)e^{ikz} + \mathcal{P}_B(z,t)e^{-ikz}\right] e^{-i\omega_{gc}t} + \text{c.c} \tag{2b}$$

assuming that the carrier frequency ω lies near the center of the lowest fundamental band gap $\omega_{gc} = kc/n_0$, where $n_0 = \epsilon_0^{1/2}$. The small detuning from the gap center $|\omega_{gc} - \omega| \ll \omega$ will be considered as phase modulation of the complex amplitude $\mathcal{E}_{F(B)}$. Under the weak-reflection assumption ($|\Delta\epsilon_m| \ll \epsilon_0$) we may drop spatially fast-varying components (varying on the scale of a wavelength) of E and $P_{\rm nl}$, and, consistently, $m > 1$ terms of $\epsilon_{\rm lin}$. We then obtain the following coupled-mode equations for the Rabi frequencies corresponding to the slow-varying field amplitudes, $\Omega_{F(B)} = \mu\mathcal{E}_{F(B)}/\hbar$, where μ is dipole moment of the TLS transition [12]

$$\left(\pm\frac{c}{n_0}\frac{\partial}{\partial z} + \frac{\partial}{\partial t}\right)\Omega_{F(B)} = ic\kappa/n_0\Omega_{B(F)} + \tau_c^{-2}\mathcal{P}_{F(B)} \tag{3}$$

Here and hereafter the upper (lower) sign corresponds to the first (second) subscript. The first term on the r.h.s. of (3) describes the forward-to-backward wave coupling via Bragg reflection with characteristic reflection (attenuation) length $1/\kappa$, where $\kappa = k\Delta\epsilon_1/4\epsilon_0$. The second term is proportional to the TLS polarization current, and $\tau_c^{-2} = (2\pi\omega_{12}\mu^2\sigma)/(n_0^2\hbar)$ is the inverse square of the cooperative resonant absorption time τ_c, σ being the density of the TLS. Note that κ is positive or negative for TLS embedded in regions with the higher or lower refractive index ($\Delta\epsilon_1 > 0$ or $\Delta\epsilon_1 < 0$), respectively.

In treatments of bidirectional field propagation in media with arbitrary spatial distribution of near-resonant atoms [13,14], the Bloch equations for the population inversion $w(z,t)$ and polarization $P_{\rm nl}$ are entangled in a fashion which leads to an infinite hierarchy of equations for successive spatial harmonics. The truncation of this hierarchy can only be justified by phenomenological arguments. Here we avoid this complication by restricting the near-resonant species distribution to thin layers (much thinner than the resonant wavelength) with the same periodicity d as the dielectric structure. Then the nonlinear polarization envelopes may be decomposed as [4]

$$\mathcal{P}_{F(B)} = \sum_j P_{\rm nl}(z_j,t)\delta(z - z_j)e^{\mp ikz} \tag{4}$$

Here $P_{\rm nl}(z_j,t)$ is the *nonlinear* polarization of the TLS in the j-th layer ($z_j = jd$). The Bloch equations then assume the form

$$\begin{aligned}\partial_t P_{\rm nl}(z_j,t) &= w(z_j,t)\left(\Omega_F e^{ikz_j} + \Omega_B e^{-ikz_j}\right) \\ &\quad - i(\omega_{gc} - \omega_{12})P_{\rm nl}(z_j,t)\end{aligned} \tag{5a}$$

$$\begin{aligned}\partial_t w(z_j,t) &= -\frac{1}{2}P_{\rm nl}^*(z_j,t)\left(\Omega_F e^{ikz_j} + \Omega_B e^{-ikz_j}\right) \\ &\quad + \text{c.c.}\end{aligned} \tag{5b}$$

where w is the population inversion and $\omega_{gc} - \omega_{12}$ is the detuning of the TLS resonance frequency ω_{12} from the gap center. The periodicity of the TLS positions which satisfy the Bragg condition, i.e., $\exp(\pm 2ikz_j) = 1$ yields $\mathcal{P}_F = \mathcal{P}_B = \mathcal{P}$ in (4). Upon summing over all layers j, the Bloch equations (5) can be written under the Bragg condition in the following closed form, without resorting to harmonic expansion

$$\partial_t \mathcal{P}(z,t) = w(z,t)\,(\Omega_F + \Omega_B) - i(\omega_{gc} - \omega_{12})\mathcal{P}(z,t) \tag{6a}$$

$$\partial_t w(z,t) = -\frac{1}{2}\left[\mathcal{P}^*(z,t)\,(\Omega_F + \Omega_B) + \text{ c.c. }\right] \tag{6b}$$

In an attempt to further simplify the Maxwell-Bloch equations, we first convert the variables to the dimensionless form $\tau = t/\tau_c$; $\zeta = n_0 z/(c\tau_c)$; $\eta = \kappa\tau_c$ and $\delta = (\omega_{gc} - \omega_{12})\tau_c$. We now rewrite Eqs.(3) and (6) for the sum and difference of the forward and backward field envelopes $\Sigma_+ = \tau_c(\Omega_F + \Omega_B)$ and $\Sigma_- = \tau_c(\Omega_F - \Omega_B)$, and obtain by simple manipulations

$$\left[\partial_\tau^2 - \partial_\zeta^2\right]\Sigma_+ = 2\partial_\tau \mathcal{P} + i2\eta\mathcal{P} - \eta^2\Sigma_+ \tag{7a}$$

$$\left[\partial_\tau^2 - \partial_\zeta^2\right]\Sigma_- = -2\partial_\zeta \mathcal{P} - \eta^2\Sigma_- \tag{7b}$$

Although Σ_+ and Σ_- now obey separate equations, they are still coupled via $\mathcal{P}$, which satisfies the Bloch equations

$$\partial_\tau \mathcal{P} = w\Sigma_+ - i\delta\mathcal{P} \tag{8a}$$

$$\partial_\tau w = -\frac{1}{2}\left(\mathcal{P}^*\Sigma_+ + \mathcal{P}\Sigma_+^*\right) \tag{8b}$$

We emphasize again the crucial role of the assumption that the TLS layers are much thinner than a wavelength and satisfy the Bragg condition. Without this assumption we could not have obtained (7) and (8), which are closed in $\mathcal{P}$ and w (in contrast to Ref. [13,14]).

Equations (7) and (8) cannot be reduced to any familiar soliton equation. Our main idea is to try for the above equations a *phase-modulated* 2π-soliton SIT solution

$$\Sigma_+ = A_0 \frac{\exp(i(\alpha\zeta - \Delta\tau))}{\cosh[\beta(\zeta/u - \tau)]} \tag{9}$$

where $\Delta = (\omega - \omega_{gc})\tau_c$, A_0 is the amplitude of the solitary pulse, β its width and u its group velocity (normalized to c).

Substituting $\partial_\tau \mathcal{P}$ from Eq.(8a) into Eq.(7a), we may express $\mathcal{P}$ in terms of Σ_+ and the population inversion w. Then, upon eliminating $\mathcal{P}$ and using Eq.(9), we can integrate Eq.(8b) for the population inversion w, obtaining

$$w = -1 - \frac{{A_0}^2(\Delta - \alpha/u)}{2(\delta - \kappa)} \frac{1}{\cosh^2[\beta(\zeta/u - \tau)]} \tag{10}$$

Using these explicit expressions for $\mathcal{P}$ and w in (7a) and (8a), we reduce our system to a set of algebraic equations for the coefficients α, Δ that determine the spatial and temporal phase modulation, and the pulse width β as functions of the velocity u. The soliton amplitude is

then found to satisfy $|A_0| = 2\beta$, exactly as in the case of usual SIT [2]. This implies, by means of Eq.(9), that the area under the Σ_+ envelope is 2π.

Let us consider the most illustrative case, when the atomic resonance is exactly at the center of the optical gap, $\delta = 0$. Then the solutions for the above parameters are [15]

$$\alpha = -\frac{\eta}{2u}\frac{1-3u^2}{1-u^2} \quad ; \quad \Delta = \frac{\eta}{2}\frac{1+u^2}{1-u^2} \tag{11a}$$

$$\beta^2 = |A_0|^2/4 = \frac{8u^2(1-u^2) - \eta^2(1+u^2)^2}{4(1-u^2)^2} \tag{11b}$$

In the frame moving with the group velocity of the pulse, $\zeta' = \zeta - u\tau$, the temporal phase modulation will be $(\alpha u - \Delta)\tau$, which is found from Eq.(11) to be equal to $-\eta\tau$. Since $\eta = \kappa\tau_c$ is the (dimensionless) gap width, this means that the frequency is detuned in the moving frame exactly to the band-gap edge. The band-gap edge corresponds (by definition) to a standing wave, whence this result demonstrates that such a pulse is indeed a soliton, which does not disperse in its group-velocity frame.

The allowed range of the solitary group velocities may be determined from Eq.(11b) through the condition $\beta^2 > 0$ for a given η, as illustrated in Fig.1. The same condition implies $|\eta| < \eta$ max, where

$$\eta^2_{\max} = \frac{8u^2(1-u^2)}{(1+u^2)^2} \tag{12}$$

It follows from (12) that the condition for SIT is $|\eta| < 1$, η max $= 1$ corresponding to $u = 1/\sqrt{3}$. This condition means that the cooperative *absorption length* $c\tau_c/n_0$ should be *shorter than the reflection* (attenuation) *length* in the gap $1/\kappa$, i.e., that the incident light should be absorbed by the TLS before it is reflected by the Bragg structure. In addition, both these lengths should be much longer than the light wavelength for the weak-reflection and slow-varying approximation to be valid.

From Eq.(7b) we find

$$\Sigma_- = \frac{1}{u}\Sigma_+ \quad , \quad \left|\Omega_{F(B)}\right| = \frac{1}{2\tau_c}\left|\left(1 \pm \frac{1}{u}\right)\Sigma_+\right| \tag{13}$$

and the equation for population inversion, obtained from Eq.(10)

$$w = -1 + \left(\frac{1}{u^2} - 1\right)\frac{\beta^2}{\cosh^2\left[\beta(\zeta/u - \tau)\right]} \tag{14}$$

The envelopes of both waves (forward and backward) propagate in the same direction; therefore the group-velocity of the backward wave is in the direction opposite to its phase-velocity! This is analogous to climbing a descending escalator.

Analogously to Kerr-nonlinear gap solitons [5,6], the real part of the nonlinear polarization $\mathrm{Re}\, P_{\mathrm{nl}}$ creates a traveling "defect" in the periodic Bragg reflector structure which allows the propagation at band-gap frequencies. The real part of the nonlinear polarization is governed by the frequency detuning from the TLS resonance. Exactly on resonance (which we here take to coincide with the gap center) $\Delta = \delta = 0$, $\mathrm{Re}\, P_{\mathrm{nl}} = 0$, and our

solutions (11) yield imaginary values of the velocity u and modulation coefficient α. The forward field envelope then decays with the same κ exponent as in the absence of TLS in the structure. Because of this mechanism, SIT exists only on one side of the band-gap center, depending on the sign of κ in Eqs.(3), i.e., on whether the TLS are in the region of the higher or the lower linear refractive index. This result may be understood as the addition of a near-resonant non-linear "refractive index" to the modulated index of refraction of the gap structure. When this addition compensates the linear modulation, then soliton propagation is possible (Fig.2). On the "wrong" side of the band-gap center, *soliton propagation is forbidden even in the allowed zone* because the nonlinear polarization then cannot compensate even for a very weak loss of the forward field due to reflection.

The soliton amplitude and velocity dependence on frequency detuning from the gap center (which coincides with atomic resonance) are illustrated in Fig.1. They demonstrate that forward soliton propagation is allowed well within the gap, for Δ satisfying $(1-\sqrt{1-\eta^2})/\eta < \Delta < (1+\sqrt{1-\eta^2})/\eta$. In addition to frequency detuning from resonance, the near-resonant gap soliton possesses another unique feature: spatial self-phase modulation $\alpha\zeta$ of both the forward and backward field components.

To check our analytical solutions (9)-(13) we have compared them with numerical simulations of Eq.(3) using the numerical method developed in [4]. As the launching condition, we take the incident wave in the form $\mathcal{E}_F = A\exp[i(\omega-\omega_{gc})(t-t_0)]/\cosh[\beta(t-t_0)/\tau_c]$ without a backward wave ($\mathcal{E}_B = 0$) at $z=0$. By varying the detuning $\omega-\omega_{gc}$ and amplitude A we investigate the field evolution inside the structure. When these parameters are close to those allowed by Eqs.(11),(12), we observe the formation and lossless propagation of both forward and backward soliton-like pulses with amplitude ratios predicted by our solutions (Fig.3.a). By contrast, exponential decay of the forward pulse in the gap is numerically obtained in the absence of TLS (Fig.3.b).

The observation of the predicted SIT at band-gap frequencies requires high values of the dipole moment μ and high density of the TLS, in order to achieve short τ_c along with large T_2 and T_1 times (to avoid dephasing and energy losses by incoherent processes). The most adequate system for experimental observation of this effect appear to be excitons in semiconductors. Let us consider a periodic array of 12-nm–thick GaAs quantum wells ($\lambda =$ 806nm) separated by $\lambda/2$ non-resonant AlGaAs layers [16]. In this system $\mu \sim 10^{-18}$cgse and area density concentration $\sigma \sim 10^8$ cm^{-2} are achievable (corresponding to an average bulk density of $\sim 10^{13}$ cm^{-3}) which yields $\tau_c \simeq 10^{-13}$s. The relaxation time (at 2^0K) is then $T_2 \sim 10$ps [16]. A solitary pulse duration of the order of $\lesssim 1$ps, i.e., much shorter then the dephasing time T_2 corresponds to a pulse width $\beta \gtrsim 0.1$. From Eq.(11) we find that SIT in this structure requires that $\eta \lesssim 0.99$, corresponding to a band-gap reflection length $1/\kappa \gtrsim 100\ \lambda$, i.e., $\Delta\epsilon_1/\epsilon_0 \lesssim 0.01$. An alternative choice may be bound I_2 excitons in CdS, which yield similar τ_c and T_2 at lower exciton densities, (controlled by the donor impurity concentration) and are therefore more appropriable for the TLS description.

To conclude, we have demonstrated the possibility of solitary pulse transmission through a one-dimensional band-gap region, by means of near-resonant polarization effects. In comparison with Kerr-nonlinear gap solitons, near-resonant gap solitons have several unique features: temporal and spatial phase modulation, the detuning conditions and the resulting velocity and amplitude threshold. Their salient advantage is stability with respect to absorption. By contrast, strong absorption is a severe problem associated with a large non-

linear Kerr coefficient. As regards applications, the sensitivity to launching conditions on the carrier frequency and pulse shape can make the predicted gap SIT an effective filter for signal transmission.

The authors are grateful to T. Lakoba, B. Sherman and M. Krongauz for useful discussions and help with the computer simulations. This work has been supported by USARDSG and the Minerva Foundation, Germany.

---

[1] S. L. McCall and E. L. Hahn, *Phys.Rev* **183**, 457 (1969); *Phys.Rev.A* **2**, 861 (1970).

[2] G. L. Lamb Jr., *Rev. Mod. Phys* **43**, 99 (1971); A. I. Maimistov, A. M. Basharov, and S. O. Elyutin, *Phys. Rep.* **191**, 2 (1990).

[3] V. I. Rupasov and V. I. Yudson, *Sov.Phys. JETP* **66**, 282 (1987); M. G. Benedict, *et. al.*, *Phys.Rev. A* **43**, 3845 (1991).

[4] B. I. Mantsyzov and R. N. Kuz'min, *Sov. Phys. JETP* **64**, 37 (1986); T. I. Lakoba and B. I. Mantsyzov, *Bulletin of the Russian Academy of Science Ph.* **56**, 1205 (1992); B. I. Mantsyzov, *ibid* **56**, 1284 (1992).

[5] W. Chen and D. L. Mills, *Phys.Rev.Lett* **58**, 160 (1987); *Phys.Rev. B* **36**, 6269 (1987).

[6] C. M. de Sterke and J. E. Sipe, *Phys.Rev. A* **38**, 5149 (1988); *ibid* **39**, 5163 (1989); *ibid* **42**, 550 (1990); M. J. Steel and C. M. de Sterke, *Phys.Rev. A* **48**, 1625 (1993).

[7] A. B. Aceves and S. Wabnitz, *Phys.Lett. A* **141**, 37 (1989).

[8] J. Feng and F. K. Kneubuhl, *IEEE Journal of Quantum Electronics* **29**, 590 (1993).

[9] M. Scalora, *et. al.*, *Phys.Rev.Lett.* **73**, 1368 (1994); *J.Appl.Phys.* **76** 2023 (1994); J. P. Dowling, *et. al.*, *J.Appl.Phys.* **75** 1896 (1994).

[10] S. L.McCall and P. M. Platzman, *IEEE Journal of Quantum Electronics* **21**, 1899 (1985).

[11] C. H. Henry, *IEEE Journal of Quantum Electronics* **21**, 1913 (1985).

[12] M. Strauss, P. Amendt, N. Rostoker, and A. Ron, *Appl. Phys. Lett* **52**, 866 (1988).

[13] M. I. Shaw and B. W. Shore, *JOSA B* **8**, 1127 (1991).

[14] R. Inguva and C. M. Bowden, *Phys.Rev.A* **41** , 1670 (1990).

[15] The lengthy analysis of the case $\delta \neq 0$ will be published elsewhere. In the limit of small δ the only stable solution (with respect to δ) from among the solutions of (11) is: $u = 1/\sqrt{3}$, $\alpha = 0$, $\Delta = \eta$ and $\beta^2 = 1 - \eta^2$, i.e., the solution which exists exactly at the band gap edge.

[16] K. Watanabe, H. Nakano, A. Honold, and Y. Yamamoto, *Phys.Rev.Lett.* **62**, 2257 (1989).

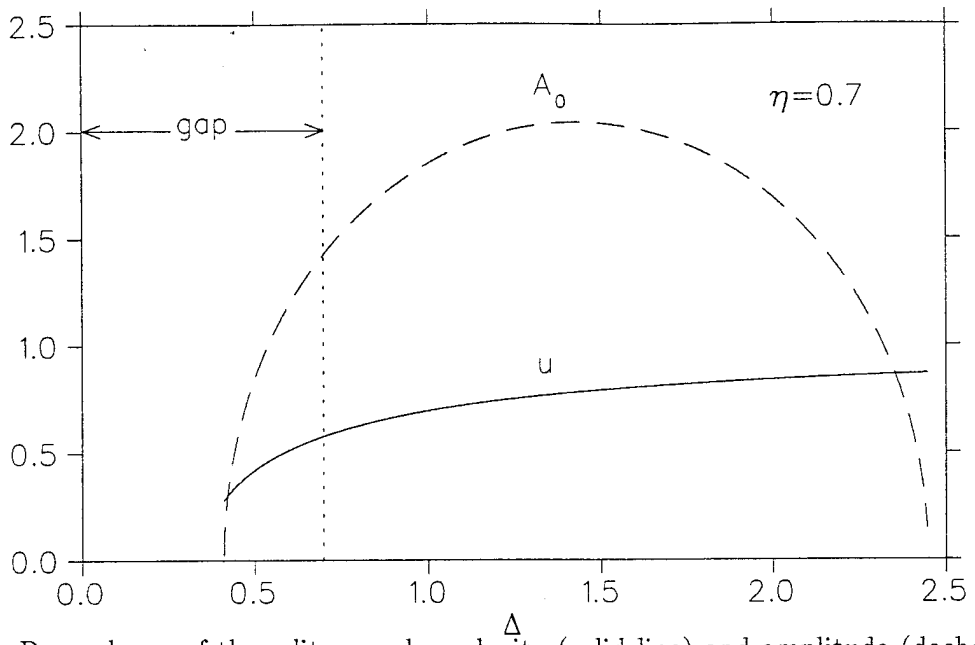

FIG. 1. Dependence of the solitary pulse velocity (solid line) and amplitude (dashed line) on frequency detuning from the gap center for $\eta = 0.7$. At the gap edge (dotted line) $u = 1/\sqrt{3}$ and $|E_F|/|E_B| = (\sqrt{3}+1)/(\sqrt{3}-1)$.

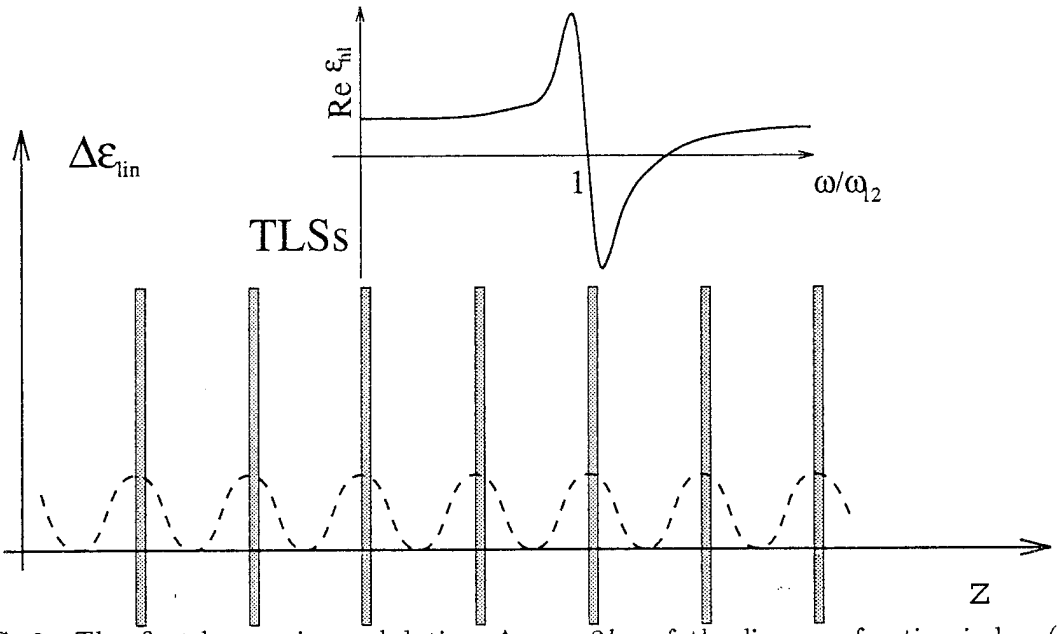

FIG. 2. The first-harmonic modulation $\Delta\epsilon_1 \cos 2kz$ of the linear refractive index (dashed curve) in a structure of periodically alternating layers. This modulation can be canceled by the near-resonant nonlinear response $Re\epsilon_{\rm nl}$ (inset), if it has the opposite sign to $\Delta\epsilon_1$ at the TLS positions.

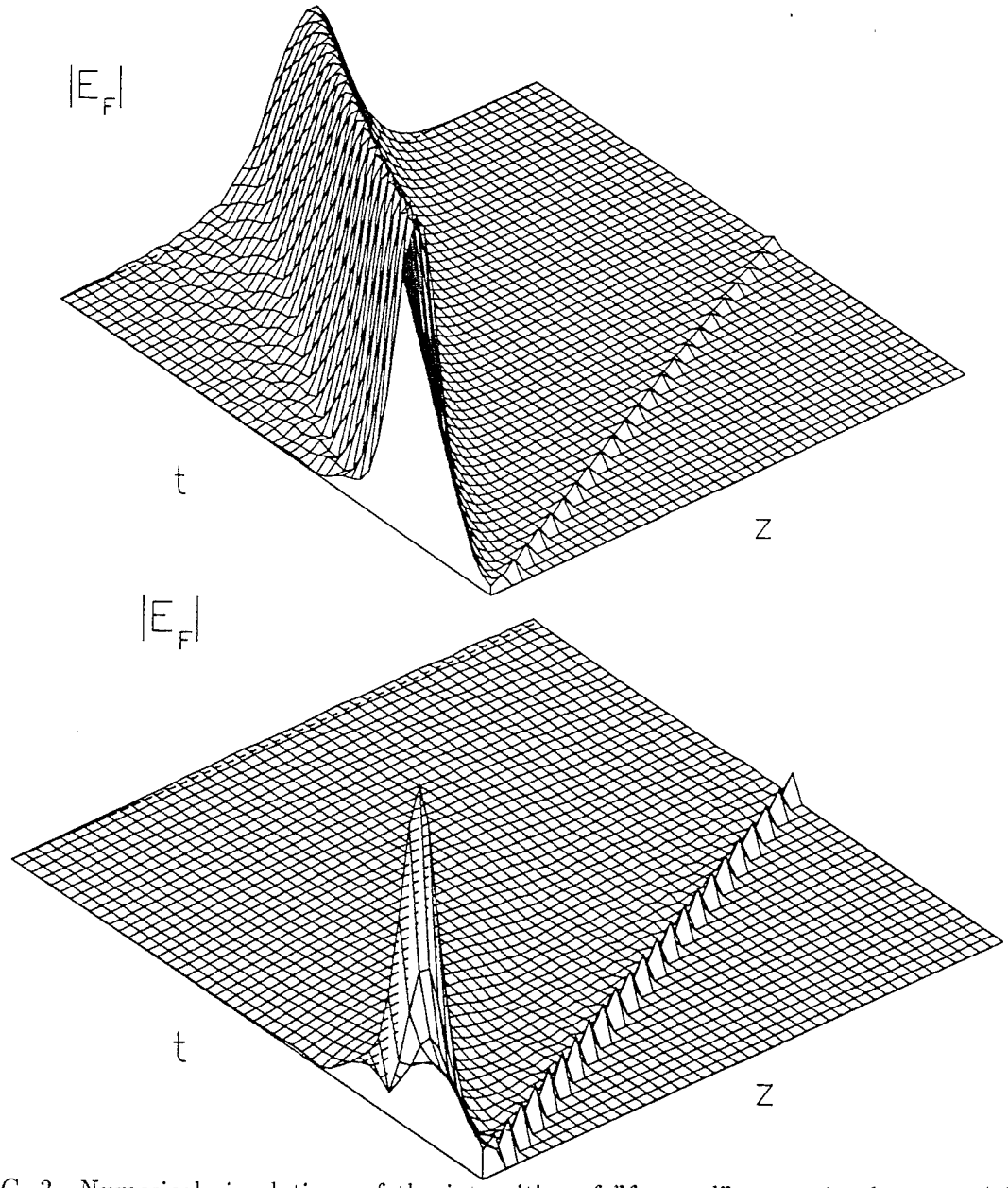

FIG. 3. Numerical simulations of the intensities of "forward" waves in the gap: (a) when Eqs.(11), (12) are obeyed ($\eta = 0.7$, group velocity $u \sim 0.3$); (b) without TLS (same η and incident pulse as in (a)).

Appendix E:
Optical "Multi-Excitons": Quantum Gap Solitons in Nonlinear Bragg Reflectors

Ze Cheng and Gershon Kurizki
Department of Chemical Physics, Weizmann Institute of Science, Rehovot 76100, Israel

We have accomplished the Bethe-ansatz solution for pairwise interacting quanta within the effective-mass regime of band-gap propagation in nonlinear Bragg reflectors. Our theory predicts a new kind of collective excitations of the electromagnetic field dressed by such media, namely, optical multi-exciton (OME) complexes (or condensates), which are the quantum states associated with gap solitary waves. Their existence should be manifested by the discrete spectrum of band-gap transmission as a function of the incident photon number and by the multi-exponential fall-off of intensity-intensity correlations on a 0.1 mm scale. OMEs should have advantageous stability properties.

Quantum effects of light propagation in nonlinear fibers have been the subject of extensive studies in recent years [1]. These studies have established that optical solitons which are classically described by the nonlinear Schrödinger equation (NLSE) [2], have quantum analogs in the form of superposition of mutually-bound (spatially-correlated) multiphoton states. The description of such bound multiphoton states is given by the Bethe ansatz solution of the second-quantized NLSE [3].

Here we address the hitherto unexplored quantum regime of optical propagation in forbidden spectral bands (band-gaps) of Kerr-nonlinear one-dimensional (1D) Bragg reflectors, wherein transmission of solitary waves (gap solitons) [4] and ultrashort pulses [5] has been predicted classically. By extending the Bethe ansatz solution to such systems, we reveal and investigate the striking analogy between mutually-bound multiphoton states of quantum gap solitons and multi-exciton complexes (excitonic molecules) in semiconductors [6]. These optical multi-excitons (OME) can be formed by the combined effect of (i) photon effective masses, which are endowed by the periodic-structure dispersion; (ii) Kerr-nonlinear interband photon attraction, and (iii) their intraband attraction or repulsion, also caused by Kerr nonlinearity. The main manifestations of OMEs are predicted here to be: (1) a series of discrete transmission lines in the optical band gap of the Bragg reflector, which correspond to increasing numbers of photon pairs and range from a single exciton to the "ionization" threshold; (2) multi-exponential fall-off of two-point intensity-intensity correlations. Both features exhibit dramatic, unparalleled dependence on the refractive-index modulation in the Bragg reflector.

The effective Hamiltonian in terms of the magnetic and electric field operators B and E in a 1D periodic Kerr-nonlinear dielectric structure can be written as

$$\hat{H} =: \int dz \left[\frac{1}{2\mu_0} B^\dagger B + \frac{\epsilon_0}{2} n^2(z) E^\dagger E + \frac{3\epsilon_0 \chi^{(3)}(z)}{4\pi\rho^2} E^\dagger E^\dagger E E \right] :, \qquad (1)$$

where : : denotes normal ordering. The Hamiltonian in Eq.(1) is similar to that used in studies of quantum solitons in nonlinear fibers [7] except that the dielectric index $n^2(z)$ and

the nonlinear susceptibility $\chi^{(3)}(z)$ are now periodic in z. Here $\pi\rho^2$ is the interaction region area, determined by the optical beam waist. On making the standard assumption that only the two bands bordering a certain band gap are involved in the nonlinear process [6], we can quantize the Hamiltonian in Eq.(1) in the two-band Bloch-function basis, denoting the lower ("valence") and upper ("conduction") bands by + and −, respectively. The quantized Hamiltonian reads

$$\hat{H} = \sum_{\alpha=\pm}\left[\sum_k \hbar\omega_{\alpha k} a^\dagger_{\alpha k} a_{\alpha k} + L^{-1}\sum_{k,k',q} V_{\alpha q}(k,k') a^\dagger_{\alpha,k'+q} a^\dagger_{\alpha,-k'} a_{\alpha,-k} a_{\alpha,k+q}\right]$$

$$+L^{-1}\sum_{k,k',q} V_{iq}(k,k') a^\dagger_{-,k'+q} a^\dagger_{+,-k'} a_{+,-k} a_{-,k+q}. \tag{2}$$

Here L is the structure length, $V_{\alpha q}(k,k')$ are the intraband matrix elements of the Kerr-nonlinear "potential", and $V_{iq}(k,k')$ are the corresponding interband matrix elements.

We are interested in photon properties near the extrema of the two bands, where $k = k_0$. We can therefore use the well-known effective-mass approximation [6]

$$\hbar\omega_{\pm k} = \hbar\omega_\pm \mp \frac{\hbar^2(k-k_0)^2}{2m_\pm}, \tag{3}$$

where $m_\pm = \mp\hbar/(\partial^2\omega_{\pm k}/\partial k^2)_{k_0}$ are the photon effective masses in the two bands. In a structure of alternating layers with refractive indices n_1, n_2 and thicknesses a_1, a_2, in the case $n_1 a_1 = n_2 a_2$ and for the second lowest band gap, the photon effective masses are found to satisfy

$$m_\pm = \mp\frac{\hbar n_1 a_1}{c(a_1+a_2)^2}\left[1+\frac{1}{2}\left(\frac{n_2}{n_1}+\frac{n_1}{n_2}\right)\right]\sin\left(\frac{2n_1 a_1 \omega_\pm}{c}\right). \tag{4}$$

One sees that $|m_- - m_+|$ scales with the band gap width when $|n_2 - n_1| \ll n_{1,2}$. Consistently with the effective-mass approximation, we replace the potential matrix elements in Eq.(2) by their values $V_\pm$ and V_i at $q = 0$ and $k = k' = k_0$. As we shall be working in the coordinate representation, we take the Fourier transform of the annihilation operators $a_{\alpha k}$, obtaining the following position-dependent field operators

$$\phi_\pm(z) = L^{-1/2}\sum_k a_{\pm k} e^{i(k-k_0)z}. \tag{5}$$

The Hamiltonian (2) can now be rewritten as

$$\hat{H} = \hbar(\omega_+ + \omega_-)\hat{N} + \hat{H}_s, \tag{6a}$$

where $\hat{N} = \int \phi^\dagger_\alpha \phi_\alpha dz$ is the single-band photon-number operator, and

$$\hat{H}_s = \int dz \left\{\sum_{\alpha=\pm}[-\alpha(\hbar^2/2m_\alpha)\partial_z\phi^\dagger_\alpha\partial_z\phi_\alpha + V_\alpha\phi^\dagger_\alpha\phi^\dagger_\alpha\phi_\alpha\phi_\alpha] + V_i\phi^\dagger_-\phi^\dagger_+\phi_+\phi_-\right\}. \tag{6b}$$

The "kinetic energy" terms depend on the structure dispersion, whereas the "potential energy" signs are those of the Kerr nonlinearity $\chi^{(3)}$, i.e., positive (negative) for self-focusing (self-defocusing) media.

Since $\hat{H}_s$ commutes with $\hat{N}$, we seek simultaneous eigenstates of both operators. Such eigenstates can be obtained exactly by the Bethe ansatz method, by extending Thacker's integrable quantum-field theory [8] to the present two-band system. Since each band contains an equal arbitrary photon number N, the Hamiltonian in Eqs.(6) admits only even numbers of quanta. We first construct the exact four-quantum eigenstate, and then generalize it to arbitrary even quantum numbers $2N$. The resulting $2N$-quantum eigenstate is obtained from a tedious calculation according to the aforementioned procedure. It is given in its unnormalized form, by

$$|\Phi_{2N}>=\int \Psi(z_{1\pm},...,z_{N\pm})\prod_{j=1}^{N}\prod_{\alpha=\pm}\left[\phi_{\alpha}^{\dagger}(z_{j\alpha})dz_{j\alpha}\right]|0>, \tag{7}$$

where the spatial envelope (wave function) is

$$\Psi(z_{1\pm},...,z_{N\pm})=\prod_{l,n=1}^{N}\left[1-\frac{im_{-}m_{+}V_i}{\hbar^2(m_{+}k_{l-}+m_{-}k_{n+})}\mathrm{sign}(z_{l-}-z_{n+})\right]$$

$$\times\prod_{\alpha=\pm}\left\{\prod_{j<l}\left[1+\alpha\frac{i2m_{\alpha}V_{\alpha}}{\hbar^2(k_{j\alpha}-k_{l\alpha})}\mathrm{sign}(z_{j\alpha}-z_{l\alpha})\right]\prod_{j=1}^{N}e^{ik_{j\alpha}z_{j\alpha}}\right\}. \tag{8}$$

The wave function $\Psi(z_{1\pm},...,z_{N\pm})$ is symmetric with respect to the exchange of any two subscripts j and l for photonic coordinates, consistently with the bosonic nature of photons. The application of the Hamiltonian $\hat{H}$ to the eigenstate $|\Phi_{2N}>$ yields the eigenenergy

$$E_{2N}=N\hbar(\omega_{+}+\omega_{-})+\sum_{j=1}^{N}\sum_{\alpha=\pm}\left(-\alpha\frac{\hbar^2k_{j\alpha}^2}{2m_{\alpha}}\right). \tag{9}$$

In the above, all the wave vectors are measured relative to the band-edge wave vector k_0.

We are looking for bound-state solutions of (8), wherein the exponential factors are real, and fall off with the separation of photons from different bands $|z_{j+}-z_{j-}|$ or from the same band, $|z_{j\alpha}-z_{j'\alpha}|$. It can be checked that the wave vectors $k_{j\alpha}$ in (8) must then satisfy

$$k_{j\pm}=\mp\frac{m_{\pm}}{m_{-}-m_{+}}K\pm i\frac{m_{-}m_{+}V_i}{(m_{-}-m_{+})\hbar^2}\mp i\frac{m_{\pm}V_{\alpha}}{\hbar^2}(N-2j+1), \tag{10}$$

where $\alpha=\pm$ is chosen according to whether the Kerr nonlinearity is positive (self-focusing) or negative (self-defocusing), and NK is the total composite momentum, which can be expressed as

$$NK=\sum_{j=1}^{N}(k_{j+}+k_{j-}). \tag{11}$$

Equation (11) indicates that bound states consist of N "excitons", i.e., pairs of "conduction"- and "valence"-band photons. On using Eqs.(10) and (11) in the wave function expression (8), we can bring it to the symmetrized form

$$\Psi(z_{1\pm},...,z_{N\pm}) \propto \exp\left(\sum_{j=1}^{N} iK\frac{m_-z_{j-}-m_+z_{j+}}{m_--m_+}\right)$$

$$\times\exp\left[-\sum_{j=1}^{N}\frac{m_-m_+V_i}{(m_--m_+)\hbar^2}|z_{j+}-z_{j-}|-\frac{|V_\alpha|}{\hbar^2}\sum_{j<l}(m_-|z_{j-}-z_{l-}|+m_+|z_{j+}-z_{l+}|)\right]. \quad (12)$$

In this expression ordering of $z_{j\pm}$'s is immaterial. The wave function (12) falls off exponentially with the distance $|z_{j+}-z_{j-}|$, under the binding condition

$$m_->m_+,\ V_i>0;\ \ m_-<m_+,\ V_i<0. \quad (13)$$

Clearly, such a wave function characterizes a bound state of N excitons, as evident from the real exponential factors and an overall translation (the first factor), analogously to a delocalized Wannier excitonic complex [6].

The exponential factors in the bound state $|\Phi_{2N}>$ can be revealed by the dependence of the intensity-intensity correlation function [3] $G^{(2)}$ on the separation η of two photon counters detecting the field in the structure:

$$G^{(2)}(\eta)=\int <\Phi_{2N}|\mathcal{E}^+(z)\mathcal{E}^-(z)\mathcal{E}^+(z+\eta)\mathcal{E}^-(z+\eta)|\Phi_{2N}>dz, \quad (14)$$

where the operator $\mathcal{E}^-(z)=\phi_+(z)+\phi_-(z)$ is the position-dependent negative-frequency field envelope. A laborious extension of the treatment in Ref.[3] to the two-band system yields $G^{(2)}(\eta)$ as a linear combination of exponential factors of the form $\exp[-(c_i+c_\pm)|\eta|]$, $\exp[-(c_++c_-)|\eta|]$ and $\exp[-(c_i+c_+/2+c_-/2)|\eta|]$, where $c_i=2m_-m_+V_i/(m_--m_+)\hbar^2$, $c_\pm=2|V_\alpha|m_\pm/\hbar^2$, and $\alpha=+$ or $-$ according to the Kerr nonlinearity sign. We have evaluated $G^{(2)}(\eta)$ for $N=2$ (a biexciton) in a periodic structure consisting of Kerr-nonlinear GaAs layers alternating with linear dielectric layers, using the linear dispersion relation from Ref.[9] and a beam spot size $\rho=0.5$ μm. The layer thicknesses are $a_1(\mathrm{GaAs})=0.2338$ μm and $a_2=0.3044$ μm. The refractive index of GaAs is $n_1=3.60$ and the refractive index n_2 of linear dielectric varies from 1.00 to 3.574. GaAs has a nonlinear susceptibility $\chi_1^{(3)}=-2.5482\times10^{-10}$ (cm/V)^2 for light frequencies below the bandgap $E_g=2.1573\times10^{15}$ s^{-1} [10]. The potentials V_i, $V_\pm$ and effective masses $m_\pm$ have been evaluated for the "conduction" and "valence" bands bordering the second lowest band gap, for which the binding condition in Eq.(12) holds (as opposed to the lowest band gap in this structure, for which this condition fails). Figure 1 clearly manifests the non-monotonic dependence of the multi-exponential fall-off of $G^{(2)}_{N=2}$ with η upon the refractive index ratio n_1/n_2. This dependence is a unique feature of the present solutions, whereas in quantum solitons traveling through Kerr-nonlinear fibers [3] the exponential fall-off of $G^{(2)}(\eta)$ depends only on the photon number N.

The bound-state energy eigenvalues are found from Eqs.(9) and (10) to have the following form,

$$E_{2N}=2N\hbar(\omega_0\pm\omega_{2N}), \quad (15)$$

$$2\hbar\omega_{2N} = \frac{\hbar^2 K^2}{2|m_- - m_+|} + \frac{m_- m_+ V_i^2}{2|m_- - m_+|\hbar^2} - \frac{|m_- - m_+|V_\pm^2}{6\hbar^2}(N^2 - 1),$$

where $\omega_0 = (\omega_+ + \omega_-)/2$ is the center of the band gap and the upper (lower) sign is chosen according to that of the Kerr nonlinearity. As seen from Eq.(15), bound states are associated with discrete transmission lines at $\Omega_{2N} = \omega_0 \pm \omega_{2N}$ in the band gap, whose progression scales quadratically with half the photon number in an incident pulse $N = \pi\rho^2\tau I_{2N}/4\hbar\Omega_{2N}$, τ being the pulse duration and I_{2N} the $2N$-photon component in the power density. We have assumed that the incident light field is in a quasi-monochromatic coherent state with band-gap frequency. Remarkably, the discreteness of the transmission spectrum will separate out different Fock states in the incident coherent state according to their relative weights, i.e., the spectrum will reflect the photon statistics! This discreteness will be revealed only if $|m_- - m_+|V_\pm^2/\hbar^2$ is spectrally resolvable, otherwise the quasiclassical limit of gap solitons will prevail. The lowest line $N = 1$, which marks the minimal transmitted intensity associated with a single exciton, is the farthest removed from the appropriate band edge, and the lines are drawn nearer to the edge as N^2 increases, as in the case of ordinary Wannier excitons [6]. However, whereas Wannier excitons have a Rydberg spectrum, with an infinite number of levels (which scale as $1/N^2$), the present bound spectrum is terminated at N_{max}, for which Eq.(15) yields $\omega_0 \pm \omega_{2N} = \omega_\pm$, marking what can be dubbed the "ionization" threshold. Since the wave vector K of excitons is measured relative to $2k_0$, the effective mass approximation requires $K \ll 2k_0$, so that we can let $K = 0$ in Eq.(15).

The spectral features discussed above are shown in Fig.2 for the same structure as in Fig.1. Here too the dependence on n_1/n_2 is strongly non-monotonic. A rather restricted range of n_1/n_2 allows the resolution of levels corresponding to different N on a 0.1 GHz scale. Using a relative refractive index $n_1/n_2 = 3.4221$ and a pulse duration $\tau = 1.0$ μs, we have obtained the transmitted intensities $I_{2N} = 8.77 \times 10^{-5}$, 3.07×10^{-3}, 7.28×10^{-3}, 8.99 and 27.41 W/cm^2, respectively, corresponding to the quantum numbers $N = 1$, 35, 83, 10^5 and 2.66×10^5, which is N_{max}. For $N > N_{max}$ the spectrum (15) is replaced by continuous bands of energy eigenvalues, embedded in the allowed "conduction" and "valence" bands. These bands are analogous to the classical "out-gap" solutions obtained above a certain intensity threshold [11].

To sum up, we have accomplished the Bethe-ansatz solution for pairwise interacting quanta within the effective-mass regime of band-gap propagation in 1D-periodic Kerr-nonlinear dielectric structures. Our theory predicts a new kind of collective excitations of the electromagnetic field dressed by such media, namely, optical multi-exciton (OME) complexes (or condensates), which are the quantum states associated with gap solitary waves. Their existence should be manifested (i) by the discrete spectrum of band-gap transmission, which reproduces the incident photon statistics, i.e., spectrally filters photon-number states on a MHz scale, and (ii) by the multi-exponential fall-off of intensity-intensity correlations on a 0.1 mm scale. Another distinct signature of OMEs is the strong non-monotonic dependence of the above properties on the periodic modulation of the refractive index in the structure.

OMEs should have advantageous stability properties, provided both linear and nonlinear absorption are negligible. The stability properties of OMEs stem from their being the exact bound eigenstates of the nonlinear field Hamiltonian which accounts for single-photon and two-photon processes in the medium. In non-absorbing media, OMEs should be sta-

ble against (a) spontaneous radiative recombination, which is the main decay mechanism of electron-hole excitons in semiconductors [6]; (b)self-focusing (-defocusing) by the Kerr nonlinearity; (c)pulse (wavepacket) dispersion and diffraction in the dielectric structure; (d)quantum fluctuations in the electromagnetic field. On the other hand, in order to ensure the OME stability against thermal scattering due to thermal fluctuations in the dielectric function, one needs low temperatures. If the dielectric structure is Raman inactive, i.e., optical phonon scattering is absent, then thermal scattering does not affect the resolution of OME lines on a 0.1 GHz scale. The ability to resolve OME lines corresponding to much lower N would necessitate band-structure design aimed at increasing the effective mass difference $|m_- - m_+|$ and the intraband nonlinear potentials $|V_\pm|$.

The support of USARDSG and the Minerva Foundation is acknowledged. One of the authors (Z. C.) is supported by the Sir Charles Clore Foundation.

---

[1] P. D. Drummond, R. M. Shelby, S. R. Friberg, and Y. Yamamoto, Nature **365**, 307 (1993), and references therein; R. Y. Chiao, I. H. Deutsch, and J. C. Garrison, Phys. Rev. Lett. **67**, 1399 (1991).

[2] A. Hasegawa, *Optical Solitons in Fibers* (Springer-Verlag, Berlin, 1990), 2nd enl. ed..

[3] Y. Lai and H. A. Haus, Phys. Rev. A **40**, 844 (1989); **40**, 854 (1989). F. X. Kärtner and H. A. Haus, Phys. Rev. A **48**, 2361 (1993).

[4] W. Chen and D. L. Mills, Phys. Rev. Lett. **58**, 160 (1987). See, for a review, C. M. de Sterke and J. E. Sipe, in *Progress in Optics*, Vol. XXXIII, edited by E. Wolf (North-Holland, Amsterdam, 1994), p. 203.

[5] M. Scalora, J. P. Dowling, C. M. Bowden, and M. J. Bloemer, Phys. Rev. Lett. **73**, 1368 (1994).

[6] H. Haug and S. Schmitt-Rink, Prog. Quant. Electr. **9**, 3 (1984).

[7] Ze Cheng, Phys. Rev. A **51**, 675 (1995).

[8] H. B. Thacker, Rev. Mod. Phys. **53**, 253 (1981).

[9] A. Yariv and P. Yeh, *Optical Waves in Crystals* (Wiley, New York, 1984), Chapter 6.

[10] J. He and M. Cada, IEEE J. Quantum Electron. **27**, 1182 (1991).

[11] J. H. Feng and F. K. Kneubühl, IEEE J. Quantum Electron. **29**, 590 (1993).

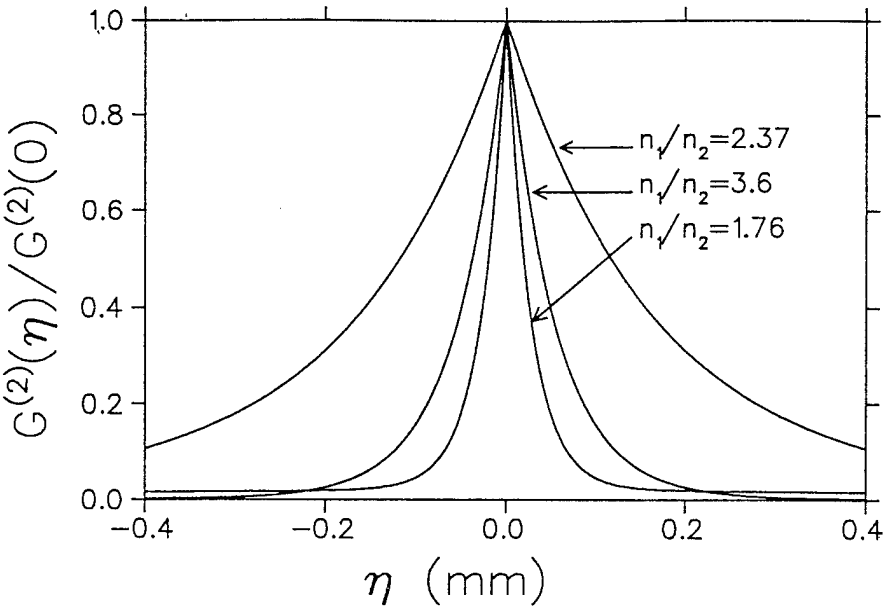

Fig. 1

FIG. 1. Dependence of the intensity correlation function $G^{(2)}(\eta)$ on the detector separation η, for the photon number $2N = 4$.

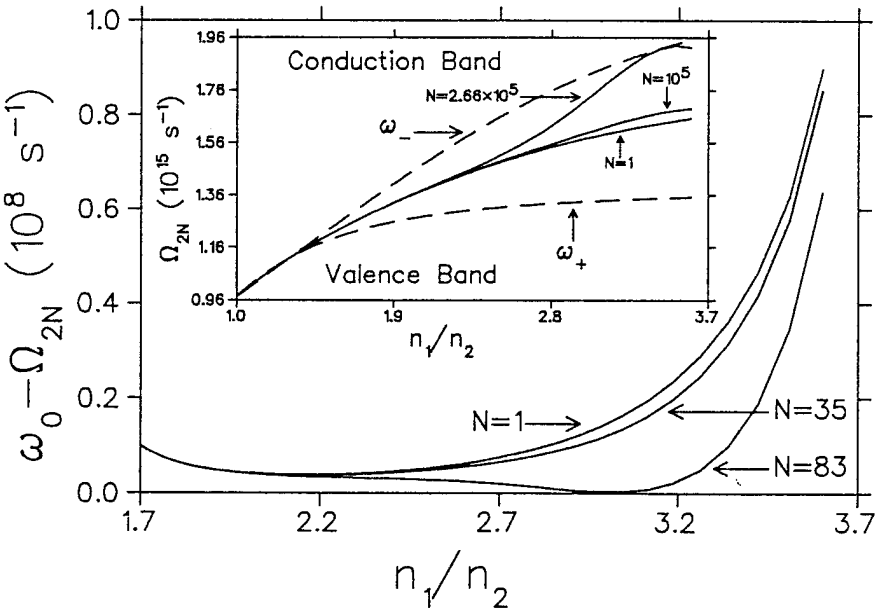

Fig. 2

FIG. 2. Variation of the optical exciton frequency Ω_{2N} with the relative refractive index n_1/n_2. The insert displays the variation of the band edges ω_+ and ω_- with n_1/n_2 and $\omega_0 = (\omega_+ + \omega_-)/2$ is the center of the band gap.

Appendix F:
Superluminal Delays of Coherent Pulses in Non-Dissipative Media: A Universal Mechanism

Y. Japha and G. Kurizki
Department of Chemical Physics, The Weizmann Institute of Science. Rehovot, Israel, 76100

We identify the universal mechanism responsible for superluminal (faster-than-light) traversal times as well as narrowing of wavepackets transmitted through various non-dissipative media. This mechanism is shown to be predominantly destructive interference between successive wavepacket components traversing all accessible causally-retarded paths. It strongly depends on wavepacket coherence and width, and can cause superluminal traversal not only in evanescent-wave "tunneling" but also in allowed propagation.

42.50.Dv, 42.50.Ar, 42.25.Md

I. INTRODUCTION

As shown by a two-photon interference experiment [1], a photon that has tunneled as an evanescent wavepacket through a dielectric-mirror "barrier" appears to have been delayed significantly less than its "twin" photon that has traversed the same distance in vacuum. Such a delay has been interpreted as signifying "superluminal" (faster-than-light) barrier-traversal time. Similar "superluminal" time delay in tunneling through a dielectric mirror has now been measured in a classical two-pulse interference experiment [2]. The latter experiment has also revealed a remarkable feature, namely, that the temporal width of the transmitted wavepacket is strongly narrowed down. These intriguing time-domain measurements add new insight to that offered by earlier spectral-domain observations of superluminal mean-phase delays, in frustrated total internal reflection [3] and waveguide transmission [4,5] of electromagnetic (EM) evanescent waves. Superluminal delays should also occur in tunneling of massive particles through potential barriers [6,7], which is analogous to EM evanescent-wavepacket transmission [8].

It is always possible to trace numerically the evanescent wavepacket evolution and compare its features with different definitions of barrier traversal times [6,7,9] (see below). Nevertheless, the *mechanism* of superluminal time delays is still obscure [1] and regarded as a "poorly resolved mystery" [9]. A commonly invoked notion is that this mechanism is spectral reshaping (filtering) of the transmitted wavepacket by dispersion. Indeed, such reshaping explains pulse narrowing and superluminal pulse traversal in absorbing [10] (or amplifying [11]) media, whose dispersion causes the faster spectral portion to be less absorbed (or more amplified) than the slower one. Analogous reshaping occurs in non-relativistic electron wavepackets which are dispersed in free space *before* hitting the barrier [9]. Yet why should spectral reshaping necessarily yield superluminal delays of EM pulses in non-absorbing structures, after propagating in (dispersionless) vacuum? Is there a *common mechanism* for superluminal time delays and wavepacket narrowing, which applies to both

EM pulses in dielectric structures and relativistic massive particles in potential barriers [4]? How is causality compatible with superluminal transmission, particularly in the single-photon case [1]?

We purport to show in this paper that the above questions can only be answered by a *universal description* of the temporal wavepacket transmission as *interference between its causally-propagating consecutive components* [12]. Our description reveals, for the first time, the key role of phase coherence in tunneling, by demonstrating its dependence on the *coherence time* (phase randomization) of the wavepacket. An important corrolary is that superluminal time delays can occur also in allowed propagation, namely, propagation which can only be described by *real wavevectors* (e.g., in Fabry-Perot structures) and not only in evanescent-wave tunneling, where complex wavevectors can be employed (e.g., in photonic band-gap structures).

II. TRANSMISSION SPECTRUM AND MEAN TRAVERSAL TIME

Our general framework assumes a classical EM pulse with field amplitude $\psi_{in}(x,t)$ that is normally incident from $x \leq 0$ onto a dielectric structure in $0 < x < L$. The field amplitude $\psi_{tr}(x,t)$ transmitted through the structure is measured at $x = L$. It is related to the incident field amplitude at $x = 0$ [13] by convolution with the impulse response $\sigma(t)$

$$\psi_{tr}(L,t) = \int_0^\infty d\tau \; \sigma(\tau) \; \psi_{in}(0, t-\tau) \tag{1}$$

where $\sigma(t)$ is the Fourier transform of the spectral transmission coefficient $\hat{\sigma}(\omega)$. The definitions of traversal times vary according to the wavepacket feature that is monitored [6,7,9]. We shall pick two of them and attempt to explain why they are superluminal, i.e., shorter than their free-space counterparts (similar explanation of other traversal times is deferred to Ref. 14): (i) The mean traversal time is defined by

$$t_{mean} = \overline{\langle t \psi_{tr}^* \psi_{tr} \rangle} \Big/ \overline{\langle \psi_{tr}^* \psi_{tr} \rangle} \tag{2}$$

where the overbar denotes integration over all times and the pointed brackets stand for an ensemble average (required for fluctuating fields). This traversal time coincides with the "center-of-gravity" arrival time [9] in the case where the propagation outside the barrier is not dispersive. We note that t_{mean} can be defined for any shape of the incident pulse. (ii) The peak traversal time, t_{peak}, can be defined if $|\psi_{tr}|$ is a smooth single-peaked function, as $\partial |\psi_{tr}(t)|^2 / \partial t|_{t=t_{peak}} = 0$. Only in the asymptotic limit of a spectrally narrow incident pulse, where the stationary phase approximation is valid, these two traversal times coincide with the so-called "phase time" [6,7] $t_{phase} = \partial\phi/\partial\omega$ where $\phi(\omega)$ is the phase of the spectral transmission function $\hat{\sigma}(\omega)$.

III. SUPERLUMINAL TRAVERSAL TIMES IN LAYERED STRUCTURES

We first show how superluminal effects occur in the simple case of a single dielectric layer: the region $0 < x < L$ is filled with a (non-dispersive) medium of refractive index n_2

and embedded in an infinite medium of refractive index n_1. The transmission coefficient $\hat{\sigma}(\omega)$ can be expanded in a series

$$\hat{\sigma}(\omega) = \sum_{j=0}^{\infty} c_j e^{i\omega\tau_j} \tag{3}$$

where each term represents a causal path, corresponding to $2j$ boundary reflections: j round trips through L followed by transmission (Fig. 1, inset). Here $\tau_j = (2j+1)n_2L/c$ is the jth path traversal time and $c_j = (1-\lambda^2)\lambda^{2j}$ are determined by the reflection amplitudes $\lambda \equiv (n_1-n_2)/(n_1+n_2)$ at the boundaries $x=0$ and $x=L$. Equation (3) also describes the transmission of a Fabry-Perot etalon (two mirrors separated by a dielectric medium) when λ is replaced by the (complex) reflection coefficient of a mirror [14]. By Fourier-transforming the expansion (3) we obtain the impulse response

$$\sigma(t) = \sum_{j=0}^{\infty} c_j \delta(t-\tau_j) \tag{4}$$

consisting of successive impulses with causal propagation times and decreasing amplitudes.

Suppose that the incident pulse $\psi_{in}(0,t)$ is of the form $\psi_{in}(0,t) = g(t)\exp[-i\xi(t)]$ where $g(t)$ is a normalized Gaussian of temporal width Δ_t and the phase $\xi(t)$ corresponds to an oscillation with frequency $\bar{\omega}$ and phase-coherence time τ_c such that $\langle e^{i\xi(t)}e^{-i\xi(t')}\rangle = e^{i\bar{\omega}(t-t')}e^{-|t-t'|/\tau_c}$. Our main tool will be the following autocorrelation function

$$\Gamma(\tau_j-\tau_k) \equiv \mathrm{Re}\overline{\langle\psi_{in}^*(t-\tau_j)\psi_{in}(t-\tau_k)\rangle} =$$

$$= \cos[\bar{\omega}(\tau_j-\tau_k)]\exp\left[-\frac{(\tau_j-\tau_k)^2}{8\Delta_t^2} - \frac{|\tau_j-\tau_k|}{\tau_c}\right] \tag{5}$$

$\Gamma(\tau_j-\tau_k)$ consists of the cosine of the relative phase between the paths i and j, weighted by an exponential term, measuring the amount of overlap and phase correlation between wavepackets traversing the two paths.

The time-integrated and ensemble-averaged transmitted intensity $I_{tr} = \overline{\langle\psi_{tr}^*\psi_{tr}\rangle}$ is expressed in term of this autocorrelation function as

$$I_{tr} = \sum_j c_j^2 + \sum_{j\neq k} c_j c_k \Gamma(\tau_j-\tau_k) \tag{6}$$

If the pulse is either very narrow ($\Delta_t \ll \tau_0$) or incoherent ($\tau_c \ll \tau_0$) then the wavepackets traveling along different paths $\tau_j \neq \tau_k$ are no longer correlated, due to phase randomization or lack of overlap. The second (coherent) term in (6) is then washed out, and the transmission becomes frequency independent. In the opposite limit, when the incident pulse is wide, smooth and coherent (transform-limited), such that $\Delta_t, \tau_c \ll \tau_0$), strong interference takes place between the different overlapping wavepackets and the second term plays a major role. When this term is large and negative, this means that the interference is strong and predominantly destructive, due to the negativity of the $\Gamma(\tau_j-\tau_k)$ terms with the largest c_jc_k weights. In the single-layer example, the transmission of a wide, transform-limited pulse becomes minimal when $\bar{\omega}(\tau_{j+1}-\tau_j)$ is an odd multiple of π, yielding $I_{tr} = [2n_1n_2/(n_1^2+n_2^2)]^2$.

The mean traversal time (Eq. (2)) through such a structure is

$$t_{mean} = \frac{1}{I_{tr}} \left\{ \sum_j c_j^2 \tau_j + \frac{1}{2} \sum_{j \neq k} c_j c_k (\tau_j + \tau_k) \Gamma(\tau_j - \tau_k) \right\} \tag{7}$$

The first (diagonal) term in (7), which is predominant for an incoherent or temporally narrow incident pulse, is always larger than the shortest causal arrival time $\tau_0 = n_2 L/c$, as expected for τ_j weighted with positive probabilities $(c_j^2 / \sum_j c_j^2)$. For a wide, coherent pulse with carrier frequency $\bar{\omega}$ such that the transmitted intensity (Eq. (6)) becomes minimal due to strong, predominantly destructive interference between the paths, the second (coherent) term in Eq. (7) can become sufficiently negative to cause $t_{mean} < \tau_0$. In the present example the minimal value of t_{mean} is $[2n_1 n_2^2/(n_1^2 + n_2^2)]L/c$, which is less than L/c if $n_2 = 1$, i.e., *superluminal*, although we deal with allowed propagation!

The width of the transmitted pulse is given by $(\Delta t)^2 = I_{tr}^{-1} \overline{\langle (t - t_{mean})^2 \psi_{tr}^* \psi_{tr} \rangle}$. It can be shown that

$$(\Delta t)^2 = \Delta_t^2 + \frac{1}{4 I_{tr}} \sum_{j,k} c_j c_k (\tau_j + \tau_k)^2 \Gamma(\tau_j - \tau_k) - t_{mean}^2 \tag{8}$$

In the limit of total incoherence, we find that $(\Delta t)^2$ is just the sum of the squared widths of the incident wavepacket Δ_t^2 and the impulse response $\sum_j \bar{c}_j^2 \tau_j^2 - (\sum_j \bar{c}_j^2 \tau_j)^2$ where $\bar{c}_j^2 = c_j^2 / \sum_j c_j^2$. In the opposite limit of strong interference between coherent and wide wavepackets $\Gamma(\tau_j - \tau_k) \sim e^{i\omega(\tau_j - \tau_k)}$. It then follows from Eqs. (5)-(7) that Eq. (8) becomes

$$(\Delta t)^2 = \Delta_t^2 - \frac{1}{4} \frac{\partial^2}{\partial \omega^2} [\ln(I_{tr}(\omega))] \Big|_{\bar{\omega}} \tag{9}$$

If $\bar{\omega}$ lies in a dip of the spectral transmission curve $I_{tr}(\omega)$ then $\partial^2 [\ln I_{tr}]/\partial \omega^2 > 0$ and the pulse will be narrowed. The temporal narrowing effect will be most salient when $\Delta_t \sim \frac{\partial^2}{\partial \omega^2} [\ln(I_{tr}(\omega))]$, provided Δ_t is large enough to allow overlap of successive wavepackets. This effect is seen to be sensitive to coherence: the phase incoherence τ_c^{-1}, which contributes only to the total spectral width of ψ_{in} and ψ_{tr} (due to the fluctuating phase $\xi(t)$), exponentially diminishing the narrowing in (8).

Figure 1 allows more insight into the case of wide and coherent ψ_{in}, for which $\psi_{tr}(L, t)$ (thick curve) consists of overlapping, destructively interfering Gaussians (thin curves). Amplitude suppression of the first transmitted wavepacket $|c_0 \psi_{in}(t - \tau_0)|$ by the next one is stronger throughout its rear half than throughout its forward half, since the envelopes $|c_j \psi_{in}(t - \tau_j)|$ with $j \geq 1$ are maximal at $t > \tau_0$. Consequently, the forward tail, which has extended through the structure already at $t < 0$, becomes the peak of ψ_{tr}, corresponding to superluminal t_{peak} and t_{mean}. Destruction of the rear half of ψ_{in} by interference also makes the transmitted pulse narrower, because it consists mostly of the forward tail of ψ_{in}. By comparison, an incoherent (fluctuating) input Gaussian of the same envelope, results in a broad, intense, $\langle |\psi_{tr}|^2 \rangle$ with *subluminal* t_{peak}.

The foregoing results render the essence of superluminal effects in the transmission through any layered structure, since the impulse response is then a discrete sum of δ-functions as in (4). Consider specifically the structure used in Refs. 1 and 2, which contains

N periods, each consisting of two layers with refractive indices n_1 and n_2, and thicknesses ℓ_1, ℓ_2. We have obtained the transmission coefficient $\hat{\sigma}_N(\omega)$ of N such periods by a recurrence relation from the single-period transmission and reflection coefficients. Its Fourier transform can be expanded, as seen from Fig. 2 (inset), in the form

$$\sigma_N(t) = \sum_{j_1,j_2=0}^{\infty} C_{j_1,j_2}^{(N)} \delta\left[t - (\tau_{j1} + \tau_{j2})\right] \tag{10}$$

Here each coefficient $C_{j_1,j_2}^{(N)}$ is the sum of the amplitudes of all possible paths traversing the n_1 and n_2 layers $N + 2j_1$ and $N + 2j_2$ times, respectively, with causal delay-times $\tau_{ji} = (N + 2j_i)n_i\ell_i/2c$ $(i = 1, 2)$. Equations (6)-(8) and the foregoing discussion of the single-layer (Fig. 1) fully apply to the multi-layered barrier, on substituting $c_j \to C_{j_1,j_2}^{(N)}$ and $\tau_j \to \tau_{j1} + \tau_{j2}$. We find that (Fig. 2) an evanescent wave is a sum of propagating transmitted waves whose leading terms interfere destructively at band gap frequencies. Correspondingly, there is constructive interference in the leading reflected waves (the Bragg reflection condition).

IV. SUPERLUMINAL TRANSMISSION TIMES IN DISPERSIVE MEDIA

The foregoing results can be extended to non-dissipative dispersive media which are characterized by a continuous impulse response, e.g., a dielectric medium with continuously varying refractive index or an optical waveguide [4,9]. The sums over paths $\sum_{j,k} c_j c_k \Gamma(\tau_j - \tau_k)$ in Eqs. (6)-(8) should be replaced by the integrals $\int d\tau \int d\tau' \sigma(\tau)\sigma(\tau')\Gamma(\tau - \tau')$. Reduced intensity, superluminal time-delay and temporal narrowing of pulses transmitted through such media follow, as in layered structures, from destructive interference between components of ψ_{tr} at different delay times $\tau \neq \tau'$, corresponding to predominantly negative contributions of $\sigma(\tau)\sigma(\tau')\Gamma(\tau - \tau')$. As an example, consider an infinite waveguide, with cutoff frequency ω_c. Its impulse response for transmission from $x = 0$ to $x = L$ has been found by us to have the causal form [15]

$$\sigma(t) = \delta(t - L/c) - \omega_c(L/c)\left[J_1(\omega_c s)/s\right]\theta(t - L/c) \tag{11}$$

where J_1 is the first-order Bessel function, θ is the Heaviside step function and $s = \sqrt{t^2 - (L/c)^2}$. If ψ_{in} is coherent and temporally wide $(\Delta_t, \tau_c \ll L/c)$ we can divide the integrals over $\sigma(\tau)\sigma(\tau')\Gamma(\tau - \tau')$ into intervals that exhibit strong cancelations in the expressions for t_{mean}, I_{tr} and $(\Delta t)^2$ (the continuous limits of Eqs. (6),(7) and (8), respectively) provided that $\bar{\omega} < \omega_c$. The superluminal delays observed in waveguide transmission below cutoff [4] are obtainable from this description. It is important that massive relativistic particles in potential barriers obeying the Klein-Gordon equation fit the same description, since their energy-momentum dispersion is the same as in light in a waveguide [8]!

V. CAUSALITY AND SIGNAL TRANSMISSION

Had the peak of the transmitted wavepacket carried any new information, its arrival after a superluminal time-delay t_{peak} would have violated causality. However, for an *analytic* input ψ_{in} in Eq. (1) the interfering forward tails of $\psi_{in}(t - \tau_j)$ which are present at $x = L$ at

$t < 0$, already contain all information on the rest of the pulse to follow. New information can only be transmitted by a *non analytic* (abrupt) disturbance of ψ_{in}, which would be causally delayed. This can be experimentally demonstrated by switching off the incident Gaussian at its peak ($t = 0$) much faster than $\bar{\omega}^{-1}$ (for $\bar{\omega}$ in the microwave range, this is achievable by a sub-picosecond optical pulse that drastically changes the transmissivity of a dielectric medium). Such abrupt switching-off corresponds to $\psi_{in}(x = 0, t) = \theta(-t)g(t)$ where $\theta(t)$ is the Heaviside step function [16]. The transmission of this ψ_{in} through any layered structure, e.g., a single-layer (Eq. (4)) yields by Eq. (1)

$$\psi_{tr}(t) = \sum_j c_j \theta(\tau_j - t) g(t - \tau_j) \tag{12}$$

The interference is unaffected by this switching-off at $t < \tau_0$. Hence, the forward half of ψ_{tr} looks the same as for an unchopped Gaussian ψ_{in} and may exhibit a superluminal t_{peak}. The true character of ψ_{in} is revealed only at $t = \tau_0 = L/c$, when the first transmitted Gaussian, $\psi_{in}(t - \tau_0)$, vanishes, causing ψ_{tr} (thick curve in Fig. 3) to drop below $|c_1 \psi_{in}(t - \tau_1)|$. This demonstrates a fundamental point: The step-like decrease at successive τ_j, transmits the switching-off information in a causal fashion, whereas superluminal features, such as t_{peak}, carry no information.

VI. PHOTON DETECTION AND SUPERLUMINAL EFFECTS

The discussion thus far has been classical, but it can easily be rendered in quantal terms, appropriate for two-photon interference [1] or one-photon detection. We must replace ψ_{in} by a field operator $\Psi_{in}^{(+)}(x, t) = \sum_\kappa a_\kappa e^{i(\kappa x - \omega(\kappa)t)}$ where a_κ are the annihilation operators of the modes κ of the free field. In the single-photon case the incident field state is $|1\rangle = \sum_\kappa g_\kappa a_\kappa^\dagger |0\rangle$ where g_κ is a Gaussian function of $\omega(\kappa)$ centered around $\bar{\omega}$ and $|0\rangle$ is the vacuum state. In this case $\Gamma(\tau_j - \tau_k)$ in Eq. (5) must be evaluated using $\langle 1|\Psi^{(-)}(x, t)\Psi^{(+)}(x', t')|1\rangle = \psi_{in}^*(x, t)\psi_{in}(x', t')$ where ψ_{in} is the classical wavepacket. Equations (6)-(8) are then valid, if I_{tr} is interpreted as the detection rate or probability of a transmitted photon. A transmitted photon is likely to be detected at "superluminal" times when its I_{tr} is peaked at the *forward tail* of the classical $|\psi_{in}(L, t)|^2$, which was *already present at the detector even at* $t < 0$. By contrast, a similar photon that has propagated the same distance through vacuum is characterized by the *peak* of $|\psi_{in}(L, t)|^2$, which arrives latter (at $t = L/c$).

VII. CONCLUSIONS

Our theory has demonstrated, for the first time, that the universal mechanism of predominantly destructive interference between accessible causal paths [12] is responsible for transmission attenuation, superluminal delay times and wavepacket narrowing. Two other characteristics of evanescent waves ,namely, exponential attenuation and traversal-length independence of t_{mean} or t_{peak} for opaque barriers [2] can also be explained in terms of this universal mechanism [15]. This theory overcomes the limitations of previous approaches, since it applies to arbitrary pulse shapes, widths and coherence times, and *explicitly* reveals the causal nature of their transmission. The understanding provided by this theory

may open new perspectives in the design of the velocity, intensity and shape of transmitted pulses, by manipulating the phase delays along the accessible paths in the medium.

This work has been supported by the Minerva Foundation, Germany and USARDSG.

---

[1] A. M. Steinberg, P. G. Kwiat and R. Y. Chiao, Phys. Rev. Lett. **71**, 708 (1993); Scientific American, August 1993, 52.

[2] Ch. Spielmann, R. Szipöcs, A. Stingl and F. Krausz, Phys. Rev. Lett. **73**, 2308 (1994)

[3] C. K. Carniglia and L. Mandel, J. Opt. Soc. Am. **61**, 1035 (1971).

[4] A. Ranfagni, D. Mugnai and A. Agresti, Phys. Lett. A **175**, 334 (1993).

[5] A. Enders and G. Nimtz, J. Phys. I (France) **3**, 1089 (1993)

[6] M. Büttiker and R. Landauer, Phys. Rev. Lett. **49**, 1739 (1982); Phys. Scr. **32**, 429 (1985). E. H. Hauge and J. A. Stovneng, Rev. Mod. Phys. **61**, 917 (1989)

[7] D. Sokolovski and L. M. Baskin, Phys. Rev. A **36**, 4604 (1987); D. Sokolovski and J. N. L. Connor, Phys. Rev. A **47**, 4677 (1993); H. A. Fertig, Phys. Rev. Lett. **65**, 2321 (1990).

[8] R. Feynman, *The Feynman Lectures on Physics*, Vol. 2, (Addison-Wesley 1977) p. 24; R. Y. Chiao, in *Analogies in Optics and Micro Electronics*, W. V. Haeringen and D. Lenstra (Kluwer 1990).

[9] T. Martin and R. Landauer, Phys. Rev A **45**, 2611 (1992).

[10] S. Chu and S. Wong, Phys. Rev. Lett. **48**, 738 (1982). The second quantized description of light propagation in absorbing media was developed by B. Huttner and S. Barnett, Phys. Rev. **A 46**, 4306 (1992)

[11] R. Y. Chiao, J. Boyce and M. W. Mitchell, Appl. Phys. B, **60**, 259 (1995)

[12] Our summation over causal paths is fundamentally different from nonrelativistic path-integral approaches [7], in which all paths are summed over, regardless of whether they represent causal or superluminal propagation.

[13] In order to avoid effects of the reflected wavepacket at $x = 0$, we can compare ψ_{tr} at $x = L$ with $\psi_{in}(x = 0)$ that has been measured in a system which has no barrier but is the same as ours for $x < 0$.

[14] G. R. Fowler, Introduction to Modern Optics (Dover, 1975) Ch. 4.

[15] Y. Japha and G. Kurizki, "Unified Causal Theory of Evanescent Wavepackets in Layered and Continuous Media" (preprint).

[16] Chopping a Gaussian wavepacket in front of a barrier was also proposed as a Gedanken experiment by J. M. Deutch and F. R. Low, Ann. Phys. **228**, 184 (1993) and discussed by A. M. Steinberg, P. G. Kwiat and R. Y. Chiao, Found. Phys. Lett. **7**, 223 (1994)

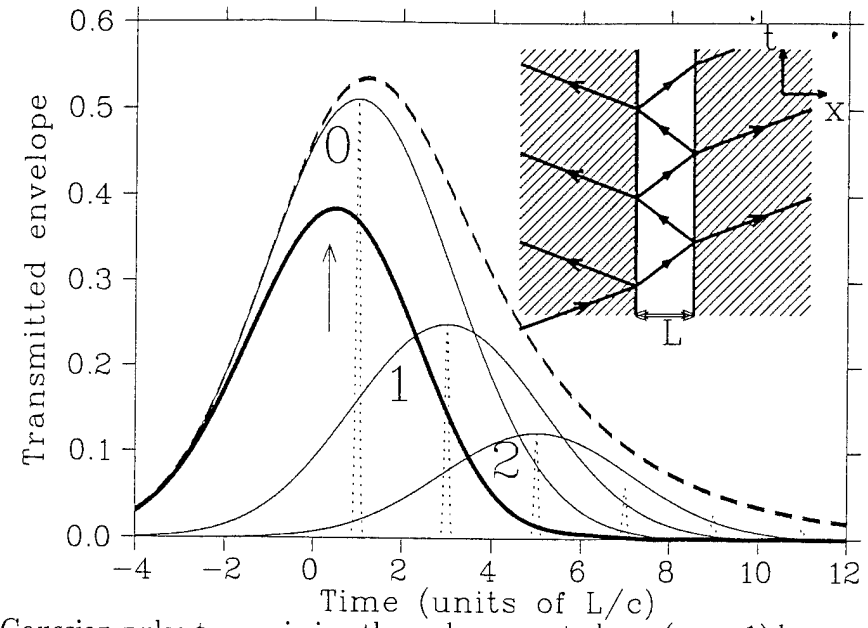

FIG. 1. A Gaussian pulse transmission through an empty layer ($n_2 = 1$) between two dielectric slabs with $n_1 = 4$. Inset - Successively transmitted terms corresponding to $2j$-fold reflections in the empty layer. Thin curves - successively transmitted Gaussians numbered by $j = 0, 1, 2, ...$ with phase delays $\bar{\omega}\tau_j = (2j+1)\pi$. Dotted curve: their coherent sum ψ_{tr} for narrow ψ_{in} ($\Delta_t = 0.03\ L/c$). Thick curve: ψ_{tr} for a wide ψ_{in} ($\Delta_t = 1.5L/c$) exhibits $t_{mean} \approx t_{peak} < L/c$ (arrow). Dashed curve: the square root of the ensemble-averaged intensity when $\tau_c = 0.5L/c$.

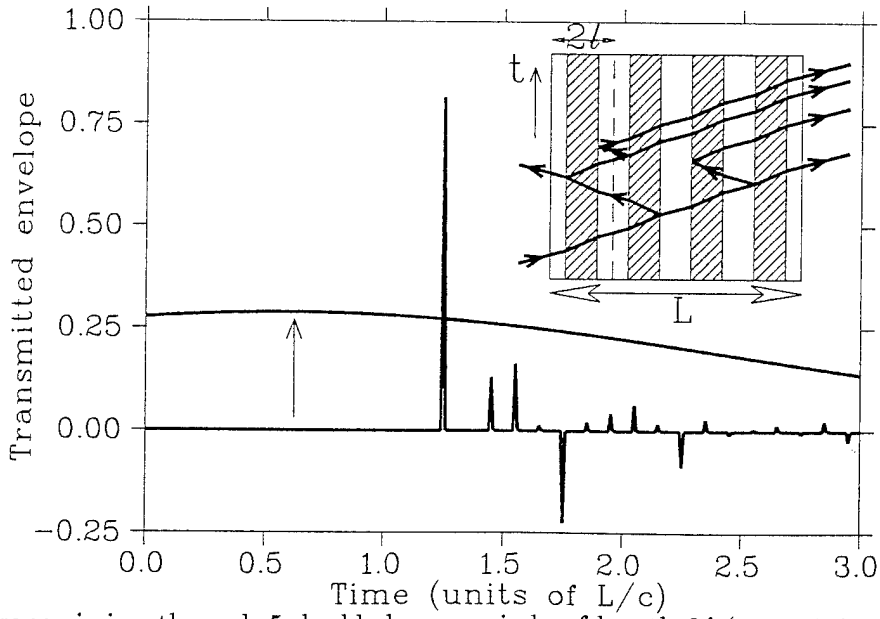

FIG. 2. Transmission through 5 double-layer periods of length 2ℓ ($n_1 = 1.5, n_2 = 1$). Inset-successively transmitted terms due to interlayer reflections. Impulse response spikes are shown at $t = \tau_{j1} + \tau_{j2}$. Solid curve: transmitted Gaussian envelope with carrier frequency $\bar{\omega}$ at the center of the band-gap and $\Delta_t = 1.5L/c$ exhibits $t_{peak} \approx 0.6L/c$.

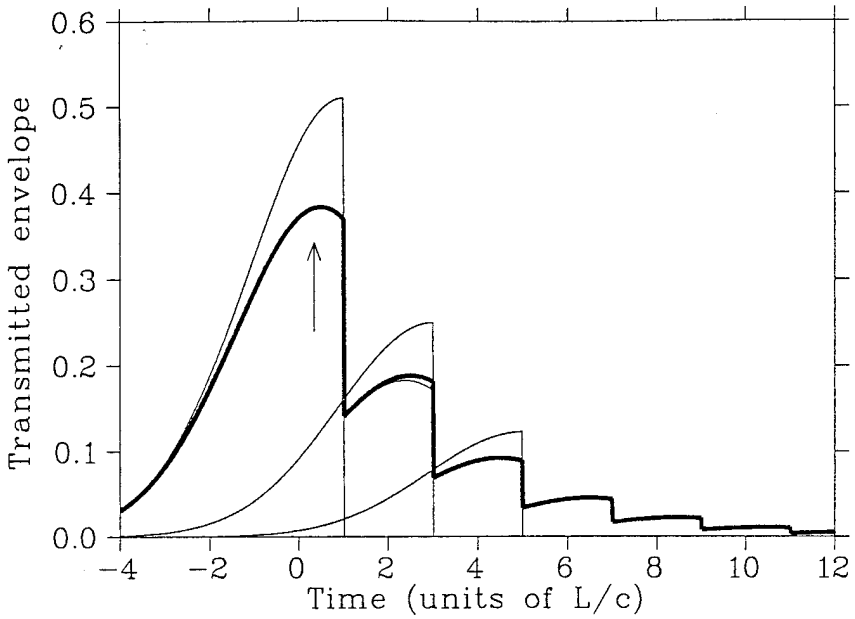

FIG. 3. Same as Fig. 1 for an incident Gaussian pulse that is chopped at $t = 0$ (Eq. (12)).